Physics Letters B 768 (2017) 103–129

Contents lists available at ScienceDirect

Physics Letters B

www.elsevier.com/locate/physletb

Multiplicity and rapidity dependence of strange hadron production in pp, pPb, and PbPb collisions at the LHC

The CMS Collaboration *

CERN, Switzerland

ARTICLE INFO

Article history:
Received 21 May 2016
Received in revised form 10 December 2016
Accepted 16 January 2017
Available online 20 February 2017
Editor: M. Doser

Keywords:
CMS
Physics
Heavy ion
Spectra
Radial flow

ABSTRACT

Measurements of strange hadron (K^0_S, $\Lambda+\overline{\Lambda}$, and $\Xi^-+\overline{\Xi}^+$) transverse momentum spectra in pp, pPb, and PbPb collisions are presented over a wide range of rapidity and event charged-particle multiplicity. The data were collected with the CMS detector at the CERN LHC in pp collisions at $\sqrt{s} = 7$ TeV, pPb collisions at $\sqrt{s_{NN}} = 5.02$ TeV, and PbPb collisions at $\sqrt{s_{NN}} = 2.76$ TeV. The average transverse kinetic energy is found to increase with multiplicity, at a faster rate for heavier strange particle species in all systems. At similar multiplicities, the difference in average transverse kinetic energy between different particle species is observed to be larger for pp and pPb events than for PbPb events. In pPb collisions, the average transverse kinetic energy is found to be slightly larger in the Pb-going direction than in the p-going direction for events with large multiplicity. The spectra are compared to models motivated by hydrodynamics.

© 2017 The Author(s). Published by Elsevier B.V. This is an open access article under the CC BY license (http://creativecommons.org/licenses/by/4.0/). Funded by SCOAP[3].

1. Introduction

Studies of strange-particle production in high energy collisions of protons and heavy ions provide important means to investigate the dynamics of the collision process. Earlier studies of relativistic heavy ion collisions at the BNL RHIC and CERN SPS colliders indicated an enhancement of strangeness production with respect to proton–proton (pp) collisions [1,2], which was historically interpreted to be due to the formation of a high-density quark–gluon medium [3]. The abundance of strange particles at different center-of-mass energies is in line with calculations from thermal statistical models [4–6]. In gold–gold (AuAu) collisions at RHIC, strong azimuthal correlations of final-state hadrons were observed, suggesting that the produced medium behaves like a near-perfect fluid undergoing a pressure-driven anisotropic expansion [2]. Studies of strangeness and light flavor production and dynamics in heavy ion collisions have provided further insight into the medium's fluid-like nature and evidence for its partonic collectivity [2,7].

In recent years, the observation of a long-range "ridge" at small azimuthal separations in two-particle correlations in pp [8] and proton-lead (pPb) [9–11] collisions with high event-by-event charged-particle multiplicity (referred to hereafter as "multiplicity") has provided an indication for collective effects in systems that are an order of magnitude smaller in size than heavy ion collisions. The nature of the observed long-range particle correlations in high multiplicity pp and pPb collisions is still under intense debate [12]. While the collective flow of a fluid-like medium provides a natural interpretation [13–16], other models attribute this behavior to the initial correlation of gluons [17–21], or the anisotropic escape of particles [22].

Studies of identified particle production and correlations in high multiplicity pp and pPb collisions provide detailed information about the underlying particle production mechanism. Identified particle (including strange-hadron) transverse momentum (p_T) spectra and azimuthal anisotropies in lead–lead (PbPb) collisions at the CERN LHC have been studied [23,24] and described by hydrodynamic models [25,26]. Similar measurements have been performed in pPb collisions as a function of multiplicity, where an indication of a common velocity boost to the produced particles, known as "radial flow" [27,28], and for a mass dependence of the anisotropic flow [29,30] have been observed. When comparing pPb and PbPb systems at similar multiplicities, a stronger radial velocity boost is seen in the smaller pPb collision system [27,30]. This could be related to a much higher initial energy density in a high multiplicity but smaller system, resulting in a larger pressure gradient outward along the radial direction, as predicted in Ref. [31]. To perform a quantitative comparison, a common average radial-flow velocity from different collision systems can be extracted from a simultaneous fit to the spectra of various particle species, based on the blast-wave model [32]. Inspired by hydrodynamics, the blast-wave model assumes a common kinetic freeze-out tempera-

* *E-mail address:* cms-publication-committee-chair@cern.ch.

http://dx.doi.org/10.1016/j.physletb.2017.01.075
0370-2693/© 2017 The Author(s). Published by Elsevier B.V. This is an open access article under the CC BY license (http://creativecommons.org/licenses/by/4.0/). Funded by SCOAP[3].

ture and radial-flow velocity for all particles during the expansion of the system. The dependence of spectral shapes for identified hadrons on the multiplicity has been observed in high energy electron and proton–antiproton collisions [33,34], but this observation was not explored extensively in the hydrodynamic context. The blast-wave fit has been studied in pp, deuterium-gold, and AuAu collisions at RHIC [35]. In pp collisions, it has been shown through studies with simulation that color reconnection processes could describe the observed multiplicity dependence of identified particle spectra [23,36].

It is of interest to study possible collective phenomena in very high multiplicity pp collisions, as demonstrated by the observation of long-range particle correlations in these events [8]. Since pp events represent an even smaller system than pPb events, a stronger radial-flow boost might be present compared to pPb and PbPb events at a comparable multiplicity [31]. Furthermore, in a pPb collision, the system is not symmetric in pseudorapidity (η). If a fluid-like medium is formed, its energy density could be different on the p- and Pb-going sides, which could lead to an asymmetry in the collective radial-flow effect as a function of η. Hydrodynamical models predict that the average p_{T} (or, equivalently, the average transverse kinetic energy $\langle \mathrm{KE_T} \rangle$, where $\langle \mathrm{KE_T} \rangle \equiv \langle m_{\mathrm{T}} \rangle - m$, with $m_{\mathrm{T}} = \sqrt{m^2 + p_{\mathrm{T}}^2}$ and m the particle mass) of produced particles is larger in the Pb-going direction than in the p-going direction, while this trend could be reversed in models based on gluon saturation [37]. Measurement of identified particle p_{T} spectra as a function of η could thus help to constrain theoretical models.

This Letter presents measurements of strange-particle p_{T} spectra in pp, pPb, and PbPb collisions as a function of the multiplicity in the events. Specifically, we examine the spectra of $\mathrm{K^0_S}$, Λ, and Ξ^- particles, where the inclusion of the charge-conjugate states is implied for Λ and Ξ^- particles. The data were collected with the CMS detector at the LHC. With the implementation of a dedicated high-multiplicity trigger, the pp and pPb data samples exhibit multiplicities comparable to that observed in peripheral PbPb collisions, where "peripheral" refers to ∼50–100% centrality, with centrality defined as the fraction of the total inelastic cross section. The most central collisions have 0% centrality. This overlap in mean multiplicity allows the three systems, with drastically different collision geometries, to be compared. The large solid-angle coverage of the CMS detector permits the strange-particle p_{T} spectra to be studied in different rapidity ranges, and thus the study of possible asymmetries with respect to the p- and Pb-going directions in pPb collisions.

2. Detector and data samples

The central feature of the CMS apparatus is a superconducting solenoid of 6 m internal diameter, which provides an axial field of 3.8 T. Within the solenoid volume are a silicon pixel and strip tracker (with 13 and 14 layers in the central and endcap regions, respectively), a lead tungstate crystal electromagnetic calorimeter (ECAL), and a brass and scintillator hadron calorimeter (HCAL), each composed of a barrel and two endcap sections. The tracker covers the pseudorapidity range $|\eta| < 2.5$. Reconstructed tracks with $1 < p_{\mathrm{T}} < 10$ GeV typically have resolutions of 1.5–3% in p_{T} and 25–90 (45–150) μm in the transverse (longitudinal) impact parameter [38]. The ECAL and HCAL each cover $|\eta| < 3.0$ while forward hadron calorimeters (HF) cover $3 < |\eta| < 5$. Muons with $|\eta| < 2.4$ are measured with gas-ionization detectors embedded in the steel flux-return yoke outside the solenoid. A more detailed description of the CMS detector, together with a definition of the coordinate system and the relevant kinematic variables, can be found in Ref. [39]. The Monte Carlo (MC) simulation of the particle propagation and detector response is based on the GEANT4 [40] program.

The data samples used in this analysis are as follows: pp collisions collected in 2010 at $\sqrt{s} = 7$ TeV, pPb collisions collected in 2013 at $\sqrt{s} = 5.02$ TeV, and PbPb collisions collected in 2011 at $\sqrt{s_{NN}} = 2.76$ TeV, with integrated luminosities of 6.2 $\mathrm{pb^{-1}}$, 35 $\mathrm{nb^{-1}}$, and 2.3 $\mathrm{\mu b^{-1}}$, respectively.

For the pPb data, the beam energies are 4 TeV for the protons and 1.58 TeV per nucleon for the lead nuclei. The data were collected in two different run periods: one with the protons circulating in the clockwise direction in the LHC ring, and one with them circulating in the counterclockwise direction. By convention, the proton beam rapidity is taken to be positive when combining the data from the two run periods. Because of the asymmetric beam conditions, the nucleon–nucleon center-of-mass in the pPb collisions moves with speed $\beta = 0.434$ in the laboratory frame, corresponding to a rapidity of 0.465. As a consequence, the rapidity of a particle in the nucleon–nucleon center-of-mass frame (y_{cm}) is detected in the laboratory frame (y_{lab}) with a shift, $y_{\mathrm{lab}} = y_{\mathrm{cm}} + 0.465$. The pPb particle yields reported in this Letter are presented in terms of y_{cm}, rather than y_{lab}, for better correspondence with the results from the pp and PbPb collisions.

3. Selection of events and tracks

The triggers, event reconstruction, and event selection are the same as those discussed for pp, pPb, and PbPb collisions in Refs. [8,41]. They are briefly outlined in the following paragraphs for pp and pPb collisions, which are the main focus of this Letter. A subset of peripheral PbPb data collected in 2011 with a minimum-bias trigger is reprocessed using the same event selection and track reconstruction algorithm as for the present pPb and pp analyses, in order to more directly compare the three systems at the same multiplicity. Details of the 2011 PbPb analysis can be found in Refs. [41,42].

Minimum-bias pPb events are triggered by requiring at least one track with $p_{\mathrm{T}} > 0.4$ GeV to be found in the pixel tracker. Because of hardware limitations in the data acquisition rate, only a small fraction ($\sim 10^{-3}$) of triggered minimum-bias events are recorded. In order to collect a large sample of high-multiplicity pPb collisions, a dedicated high-multiplicity trigger is implemented using the CMS Level-1 (L1) and high-level trigger (HLT) systems [43]. At L1, the total transverse energy summed over the ECAL and HCAL is required to exceed either 20 or 40 GeV, depending on the multiplicity requirement as specified below. Charged particles are reconstructed at the HLT level using the pixel detectors. It is required that these tracks originate within a cylindrical region (30 cm in length along the direction of the beam axis and 0.2 cm in radius in the direction perpendicular to that axis) centered on the nominal interaction point. For each event, the number of pixel tracks ($N_{\mathrm{trk}}^{\mathrm{online}}$) with $|\eta| < 2.4$ and $p_{\mathrm{T}} > 0.4$ GeV is determined for each reconstructed vertex. Only tracks with a distance of closest approach 0.4 cm or less to one of the vertices are included. The HLT selection requires $N_{\mathrm{trk}}^{\mathrm{online}}$ for the vertex with the largest number of tracks to exceed a specific value. Data are collected in pPb collisions with thresholds $N_{\mathrm{trk}}^{\mathrm{online}} > 100$ and 130 for events with an L1 transverse energy threshold of 20 GeV, and $N_{\mathrm{trk}}^{\mathrm{online}} > 160$ and 190 for events with an L1 threshold of 40 GeV. While all events with $N_{\mathrm{trk}}^{\mathrm{online}} > 190$ are accepted, only a fraction of the events from the other thresholds are retained. This fraction is dependent on the instantaneous luminosity. Data from both the minimum-bias trigger and the high-multiplicity trigger are retained for offline analysis. Similar high-multiplicity triggers, with different thresholds, were developed for pp collisions, with details given in Ref. [8].

In the subsequent analysis of all collision systems, hadronic events are selected by requiring the presence of at least one energy deposit larger than 3 GeV in each of the two HF calorimeters. Events are also required to contain a primary vertex within 15 cm of the nominal interaction point along the beam axis and 0.15 cm in the transverse direction, where the primary vertex is the reconstructed vertex with the largest track multiplicity. At least two reconstructed tracks are required to be associated with this primary vertex, a condition that is important only for minimum-bias events. Beam-related background is suppressed by rejecting events in which less than 25% of all reconstructed tracks satisfy the high-purity selection defined in Ref. [38]. In the pPb data sample, there is a 3% probability to have at least one additional interaction in the same bunch crossing (pileup). The procedure used to reject pileup events in pPb collisions is described in Ref. [41]. It is based on the number of tracks associated with each reconstructed vertex and the distance between different vertices. A purity of 99.8% for single pPb collision events is achieved for the highest multiplicity pPb range studied in this Letter. For the pp data, the average number of collisions per bunch crossing is 1.2. However, pp interactions that are well separated from each other do not interfere. Thus, among events identified as containing pileup, the event is retained if the separation between the primary vertex and any other vertex exceeds 1 cm. In such events, only tracks from the highest multiplicity vertex are used.

With the above criteria, 97% (98%) of the simulated pPb events generated with the EPOS LHC [44] (HIJING 2.1 [45]) programs are selected. Similarly, 94% (96%) of the pp events simulated with the PYTHIA 6 Tune Z2 [46] (PYTHIA 8 Tune 4C [47]) programs are selected.

The event-by-event charged-particle multiplicity $N_{\mathrm{trk}}^{\mathrm{offline}}$ is defined using primary tracks, i.e., tracks that satisfy the high-purity criteria of Ref. [38] and, in addition, the following criteria designed to improve track quality and ensure the tracks emanate from the primary vertex. The impact parameter significance of the track with respect to the primary vertex in the direction along the beam axis, $d_z/\sigma(d_z)$, is required to be less than 3, as is the corresponding impact parameter in the transverse plane, $d_{\mathrm{T}}/\sigma(d_{\mathrm{T}})$. The relative p_{T} uncertainty, $\sigma(p_{\mathrm{T}})/p_{\mathrm{T}}$, must be less than 10%. To ensure high tracking efficiency and to reduce the rate of misreconstructed tracks, the tracks are required to satisfy $|\eta| < 2.4$ and $p_{\mathrm{T}} > 0.4$ GeV. Based on simulated samples generated with the HIJING program, the efficiency for primary track reconstruction is found to be greater than 80% for charged particles with $p_{\mathrm{T}} > 0.6$ GeV and $|\eta| < 2.4$. For the multiplicity range studied in this Letter, no dependence of the tracking efficiency on multiplicity is found and the rate of misreconstructed tracks is 1–2%.

The pp, pPb, and PbPb data are divided into classes based on $N_{\mathrm{trk}}^{\mathrm{offline}}$. The quantity $N_{\mathrm{trk}}^{\mathrm{corrected}}$ is the corresponding multiplicity corrected for detector and algorithm inefficiencies in the same kinematic region ($|\eta| < 2.4$ and $p_{\mathrm{T}} > 0.4$ GeV). The fraction of the total multiplicity found in each interval and the average number of tracks both before and after accounting for the corrections are listed in Table 1 for the pp data and in Ref. [41] for the pPb and PbPb data. The uncertainty in the average value $\langle N_{\mathrm{trk}}^{\mathrm{corrected}} \rangle$ is evaluated from the uncertainty in the tracking efficiency, which is 3.9% for a single track [48]. For the pp data, six multiplicity intervals, indicated in Table 1, are defined, which are inclusive for the lower bounds and exclusive for the upper bounds, as indicated in Table 1. The average $N_{\mathrm{trk}}^{\mathrm{offline}}$ value of minimum-bias events is similar to that for the multiplicity range $N_{\mathrm{trk}}^{\mathrm{offline}} < 35$. For the pPb and PbPb data, eight intervals are defined. These eight intervals are indicated, e.g., in the legend of Fig. 2. Note that, unlike pp and PbPb collisions, $N_{\mathrm{trk}}^{\mathrm{offline}}$ for pPb collisions is not determined in the center-of-mass frame. However, the difference in the $N_{\mathrm{trk}}^{\mathrm{offline}}$ definition between the laboratory and the center-of-mass frames is found to be minimal and so this difference is ignored. The detector condition has been checked to be stable for events with different multiplicities.

Table 1
Fraction of the full event sample in each multiplicity interval and the average multiplicity per interval for pp data. The multiplicities $N_{\mathrm{trk}}^{\mathrm{offline}}$ and $N_{\mathrm{trk}}^{\mathrm{corrected}}$ are determined for $|\eta| < 2.4$ and $p_{\mathrm{T}} > 0.4$ GeV before and after efficiency corrections, respectively. The third and fourth columns list the average values of $N_{\mathrm{trk}}^{\mathrm{offline}}$ and $N_{\mathrm{trk}}^{\mathrm{corrected}}$.

Multiplicity interval ($N_{\mathrm{trk}}^{\mathrm{offline}}$)	Fraction	$\langle N_{\mathrm{trk}}^{\mathrm{offline}} \rangle$	$\langle N_{\mathrm{trk}}^{\mathrm{corrected}} \rangle$
[0, 35)	0.93	12	14 ± 1
[35, 60)	0.06	43	50 ± 2
[60, 90)	6×10^{-3}	68	79 ± 3
[90, 110)	2×10^{-4}	97	112 ± 4
[110, 130)	1×10^{-5}	116	135 ± 5
[130, ∞)	7×10^{-7}	137	158 ± 6

4. The K_S^0, Λ, and Ξ^- reconstruction and yields

The reconstruction and selection procedures for K_S^0, Λ, and Ξ^- candidates are presented in Refs. [30,49]. To increase the efficiency for tracks with low momenta and large impact parameters, both characteristic of the strange-particle decay products, the loose selection of tracks, as defined in Ref. [38], is used. The K_S^0 and Λ candidates (generically referred to as "V^0s") are reconstructed, by combining oppositely charged particles to define a secondary vertex. Each of the two tracks must have hits in at least four layers of the silicon tracker, and transverse and longitudinal impact parameter significances with respect to the primary vertex greater than 1. The distance of closest approach of the pair of tracks to each other is required to be less than 0.5 cm. The fitted three-dimensional vertex of the pair of tracks is required to have a χ^2 value divided by the number of degrees of freedom less than 7. Each of the two tracks is assumed to be a pion in the case of the K_S^0 reconstruction. As the proton carries nearly all of the momentum in the Λ decay, the higher-momentum track is assumed to be a proton and the other track a pion in the case of the Λ reconstruction. To reconstruct Ξ^- particles, a Λ candidate is combined with an additional charged particle carrying the correct sign, to define a common secondary vertex. This additional track is required to have hits in at least four layers of the silicon tracker, and both the transverse and longitudinal impact parameter significances with respect to the primary vertex are required to exceed 3.

Due to the long lifetime of the K_S^0 and Λ particles, the significance of the V^0 decay length, which is the three-dimensional distance between the primary and V^0 vertices divided by its uncertainty, is required to exceed 5. To remove K_S^0 candidates misidentified as Λ particles and vice versa, the Λ (K_S^0) candidate mass assuming both tracks to be pions (the lower-momentum track to be a pion and the higher-momentum track a proton) must differ by more than 20 (10) MeV from the nominal [50] K_S^0 (Λ) mass value. To remove photon conversions to an electron–positron pair, the mass of a K_S^0 or Λ candidate assuming both tracks to have the electron mass must exceed 15 MeV. The angle θ^{point} between the V^0 momentum vector and the vector connecting the primary and V^0 vertices is required to satisfy $\cos\theta^{\mathrm{point}} > 0.999$. This reduces the contributions of particles from nuclear interactions, random combinations of tracks, and secondary Λ particles originating from the weak decays of Ξ and Ω particles.

To optimize the reconstruction of Ξ^- particles, requirements on the three-dimensional impact parameter significance of its decay products with respect to the primary vertex are applied. This significance must be larger than 3 (4) for the proton (pion) tracks

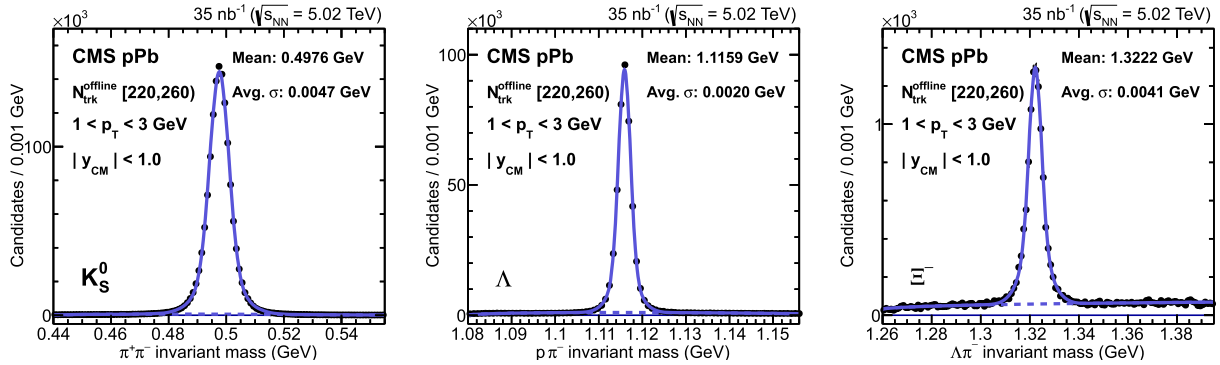

Fig. 1. Invariant mass distribution of K_S^0 (left), Λ (middle), and Ξ$^-$ (right) candidates in the p_T range 1–3 GeV for $220 \le N_{trk}^{offline} < 260$ in pPb collisions. The inclusion of the charge-conjugate states is implied for Λ and Ξ$^-$ particles. The solid lines show the results of fits described in the text. The dashed lines indicate the fitted background component.

from the Λ decay, and larger than 5 for the direct pion candidate from the Ξ$^-$ decay. To further reduce the background from random combinations of tracks, the corresponding impact parameter significance of Ξ$^-$ candidates cannot exceed 2.5. The three-dimensional decay length significance, with respect to the primary vertex, of the Ξ$^-$ candidate and the associated Λ candidate must exceed 3 and 12, respectively.

The K_S^0, Λ, and Ξ$^-$ reconstruction efficiencies are about 15, 5, and 0.7% for $p_T \approx 1$ GeV, and 20, 10, and 2% for $p_T > 3$ GeV, averaged over $|\eta| < 2.4$. These efficiencies account for the effects of acceptance, and for the branching fractions of the decay modes in which the strange particles are reconstructed. The invariant mass distributions of reconstructed K_S^0, Λ, and Ξ$^-$ candidates with $1 < p_T < 3$ GeV are shown in Fig. 1 for pPb events with $220 \le N_{trk}^{offline} < 260$. Prominent mass peaks are visible, with little background. The solid lines show the result of a maximum likelihood fit. In this fit, the strange-particle peaks are modeled as the sum of two Gaussian functions with a common mean. The "average σ" values in Fig. 1 are the square root of the weighted average of the variances of the two Gaussian functions. The background is modeled with a quadratic function for the K_S^0 results, with the analytic form $Aq^{1/2} + Bq^{3/2}$ with $q = m - (m_\pi + m_p)$ for the Λ results, and with the form Cq^D with $q = m - (m_\Lambda + m_\pi)$ for the Ξ$^-$ results, where A, B, C, and D are fitted parameters. These fit functions are found to provide a good description of the signal and background with relatively few free parameters. The fits are performed over the ranges of strange-particle invariant masses indicated in Fig. 1 to obtain the raw strange-particle yields $N^{raw}_{K_S^0/\Lambda/\Xi^-}$.

The raw strange-particle yields are corrected to account for the branching fraction of the reconstructed decay mode, and for the acceptance and reconstruction efficiency of the strange particle, using simulated event samples based on the PYTHIA 6 (pp) or EPOS (pPb and PbPb) event generator and GEANT4 modeling of the detector:

$$N^{corr}_{K_S^0/\Lambda/\Xi^-} = \frac{N^{raw}_{K_S^0/\Lambda/\Xi^-}}{R_{corr}}, \tag{1}$$

where R_{corr} is a correction factor from simulation given by the ratio of the raw reconstructed yield to the total generated yield for the respective strange particle, with $N^{corr}_{K_S^0/\Lambda/\Xi^-}$ the corrected yield.

The raw Λ particle yield includes contributions from the decays of Ξ$^-$ and Ω particles. This "nonprompt" contribution is largely determined by the relative Ξ$^-$ to Λ yield (because the contribution from Ω particles is negligible). The stringent requirements placed on $\cos\theta^{point}$ remove a large fraction of the nonprompt Λ component but, from simulation, up to 10% of the Λ candidates at high p_T are nonprompt. If the relative Ξ$^-$ to Λ yield in simulation is modeled precisely, the contamination from nonprompt Λ particles will be removed by the correction procedure of Eq. (1). Otherwise, an additional correction to account for the residual contamination is necessary. As the Ξ$^-$ particle yields are explicitly measured in this analysis, this residual correction factor can be determined directly from the data as:

$$f^{residual}_{\Lambda,np} = 1 + f^{raw,MC}_{\Lambda,np}\left(\frac{N^{corr}_{\Xi^-}/N^{corr}_{\Lambda}}{N^{MC}_{\Xi^-}/N^{MC}_{\Lambda}} - 1\right), \tag{2}$$

where $f^{raw,MC}_{\Lambda,np}$ denotes the fraction of nonprompt Λ particles in the raw reconstructed Λ sample as determined from simulation, while $N^{corr}_{\Xi^-}/N^{corr}_{\Lambda}$ and $N^{MC}_{\Xi^-}/N^{MC}_{\Lambda}$ are the Ξ$^-$-to-Λ yield ratios from the data after applying the corrections of Eq. (1), and from generator-level simulation, respectively. The final prompt Λ particle yield is given by $N^{corr}_{\Lambda}/f^{residual}_{\Lambda,np}$. Based on EPOS MC studies, which has a similar Ξ^-/Λ ratio to the data, the residual nonprompt contributions to the Λ yields are found to be negligible in pPb and PbPb collisions, while in pp collisions the correction is 1–3% depending on the p_T value of the Λ particle. Note that N^{corr}_{Λ} in Eq. (2) is derived using Eq. (1), which in principle contains the residual nonprompt Λ contributions. Nonetheless, by applying Eq. (2) in an iterative fashion, we expect N^{corr}_{Λ} to approach a result corresponding to prompt Λ particles only. A second iteration of correction is found to have an effect of less than 0.1% on the Λ particle yield. As a cross-check we treat the sample of simulated events generated with the HIJING program like data and verify that we obtain the correct yields at the generator level after applying the correction procedure described above.

5. Systematic uncertainties

Table 2 summarizes the different sources of systematic uncertainty in the yields of each strange particle species. The values in parentheses correspond to the systematic uncertainties in the forward rapidity regions ($-2.4 < y_{cm} < -1.5$ and $0.8 < y_{cm} < 1.5$) for pPb data, if they differ from those at mid-rapidity. The dominant sources of systematic uncertainty are associated with the strange-particle reconstruction, especially the efficiency determination.

The systematic uncertainty in determining the efficiency of a single track is 3.9% [48]. The tracking efficiency is strongly correlated with the lifetime of a particle because when and where a particle decays determine how efficiently the detector captures its decay products. We observe agreement of the K_S^0 lifetime distribution ($c\tau$) between data and simulation, and similarly for the

Table 2
Summary of systematic uncertainties for the p_T spectra of K^0_S, Λ, and Ξ^- particles in the center-of-mass rapidity range $|y_{cm}| < 1.0$ (for pPb events, at forward rapidities, if different) for the three collision systems.

Source	K^0_S (%)		Λ (%)		Ξ^- (%)
p_T (GeV)	<1.5	>1.5	<1.5	>1.5	
Single-track efficiency	7.8	7.8	7.8	7.8	11.7
Yield extraction	2 (3)	2 (3)	2 (4)	2 (4)	3
Selection criteria	3.6 (3.6)	2.2 (3.6)	3.6 (6.4)	2.2 (6.4)	7
Momentum resolution	2	2	2	2	2
Nonprompt Λ correction			2	2	
Pileup (pp only)	3	1	3	1	3
Proton direction (pPb only)	3 (3)	3 (3)	3 (5)	3 (5)	4
Rapidity binning	1 (2)	1 (2)	1 (3)	1 (3)	2
Efficiency correction					5
Total (pp)	9.6	8.7	9.8	8.9	15.4
Total (pPb)	9.6 (10.0)	9.2 (10.0)	9.8 (12.6)	9.4 (12.6)	15.6
Total (PbPb)	9.1	8.6	9.3	8.9	15.1

Λ and Ξ^-, which provides a cross-check of the systematic uncertainty. This translates into a systematic uncertainty in the reconstruction efficiency of 7.8% for the K^0_S and Λ particles, and 11.7% for the Ξ^- particles. Different background fit functions and methods to extract the yields for the K^0_S, Λ, and Ξ^- are compared. The background fit function is varied to a fourth-order polynomial for the K^0_S and Λ studies, and to a linear function for the Ξ^- study. The yields are obtained by integrating over a region that is ± 5 times the average resolution and centered at the mean, rather than over the entire fitted mass range. Possible contamination by residual misidentified V^0 candidates (i.e., a K^0_S particle misidentified as a Λ particle, or vice versa) is investigated by varying the invariant mass range used to reject misidentified V^0 candidates. On the basis of these studies we assign systematic uncertainties of 2–4% to the yields. Systematic effects related to the selection of the strange-particle candidates are evaluated by varying the selection criteria, resulting in an uncertainty of 1–7%. The impact of finite momentum resolution on the spectra is estimated using the EPOS event generator. Specifically, the generator-level p_T spectra of the strange particles are smeared by the momentum resolution, which is determined through comparison of the generator-level and matched reconstructed-level particle information. The difference between the smeared and original spectra is less than 2%. The systematic uncertainty associated with nonprompt Λ corrections to the Λ spectra is evaluated through propagation of the systematic uncertainty in the $N^{corr}_{\Xi^-}/N^{corr}_{\Lambda}$ ratio in Eq. (2) to the $f^{residual}_{\Lambda,np}$ factor, and is found to be less than 2%. Systematic uncertainties introduced by possible residual pileup effects for pp data are estimated to be 1–3%. This uncertainty is evaluated through both tightening (only one reconstructed vertex allowed per event) and loosening (no event rejection on the basis of the number of vertices) the pileup rejection criteria [41]. The uncertainty associated with pileup is negligible for the pPb and PbPb data since there are very few events in those samples with more than one reconstructed vertex. In pPb collisions, the direction of the p and Pb beams were reversed during course of the data collection, as mentioned in Section 2. Comparison of the particle p_T spectra with and without the beam reversal yields an uncertainty of 2–5% for all particle types. The effect of the choice of the rapidity bins is assessed by dividing each bin into two, thereby doubling the number of bins, resulting in a systematic uncertainty of 1–3% for the p_T spectra. For the Ξ^-, the reconstruction efficiency correction is smoothed by averaging adjacent bins in order to compensate for the limited statistical precision of the MC sample. Variations in the smoothing procedure lead to a systematic uncertainty of 5% for the p_T spectra of the Ξ^-.

All sources of systematic uncertainty are uncorrelated and summed in quadrature to define the total systematic uncertainties in the p_T spectra of each strange particle. The total systematic uncertainties between the pp, pPb, and PbPb systems are similar and largely correlated. When calculating ratios of particle yields, most of the systematic uncertainties partially or entirely cancel. For example, the systematic uncertainties due to tracking efficiency and pileup for the $\Lambda/2K^0_S$ ratio are negligible.

6. Results

6.1. Multiplicity dependence at mid-rapidity

The p_T spectra of K^0_S, Λ, and Ξ^- particles with $|y_{cm}| < 1$ in pp collisions at $\sqrt{s} = 7$ TeV (top), pPb collisions at $\sqrt{s} = 5.02$ TeV (middle), and PbPb collisions at $\sqrt{s_{NN}} = 2.76$ TeV (bottom) are presented in Fig. 2, for different multiplicity intervals. Due to details in the implementation of the dedicated high-multiplicity trigger thresholds used to select the pp events, the multiplicity intervals for pp events differ slightly from those for pPb and PbPb events. The p_T differential yield is defined as $d^2N/(2\pi p_T)dp_T dy$. For the purpose of better visibility, the data are scaled by factors of 2^{-n}, as indicated in the figure legend. A clear evolution of the spectral shape with multiplicity can be seen for each particle species in each collision system. For higher multiplicity events, the spectra tend to become flatter (i.e., "harder"), indicating a larger $\langle KE_T \rangle$ value. Within each collision system, heavier particles (e.g., Ξ^-) exhibit a harder spectrum than lighter particles (K^0_S), especially for high-multiplicity events.

To examine the differences in the multiplicity dependence of the spectra in greater detail, the ratios $\Lambda/2K^0_S$ and Ξ^-/Λ of the yields are shown in Fig. 3 as a function of p_T for different multiplicity ranges in the pp, pPb, and PbPb systems. The results for the $\Lambda/2K^0_S$ ratio are shown in Fig. 3 (top). For $p_T \lesssim 2$ GeV, the $\Lambda/2K^0_S$ ratio is seen to be smaller in high-multiplicity events than in low-multiplicity events for a given p_T value. In pp and pPb collisions, this trend is similar to what has been observed between peripheral and central PbPb collisions [23]; this trend is not as evident for the PbPb data in Fig. 3 (top right) because in the present study only PbPb events of 50–100% centrality are considered. At higher p_T, this multiplicity ordering of the $\Lambda/2K^0_S$ ratio is reversed. In hydrodynamic models such as those presented in Refs. [51,52], this behavior can be interpreted as the effect of radial flow. A stronger radial flow is developed in higher-multiplicity events, which boosts heavier particles (e.g., Λ) to higher p_T, resulting in a suppression of the $\Lambda/2K^0_S$ ratio at low p_T. Comparing the various collision systems at low p_T, the difference in the $\Lambda/2K^0_S$ ratio between low-

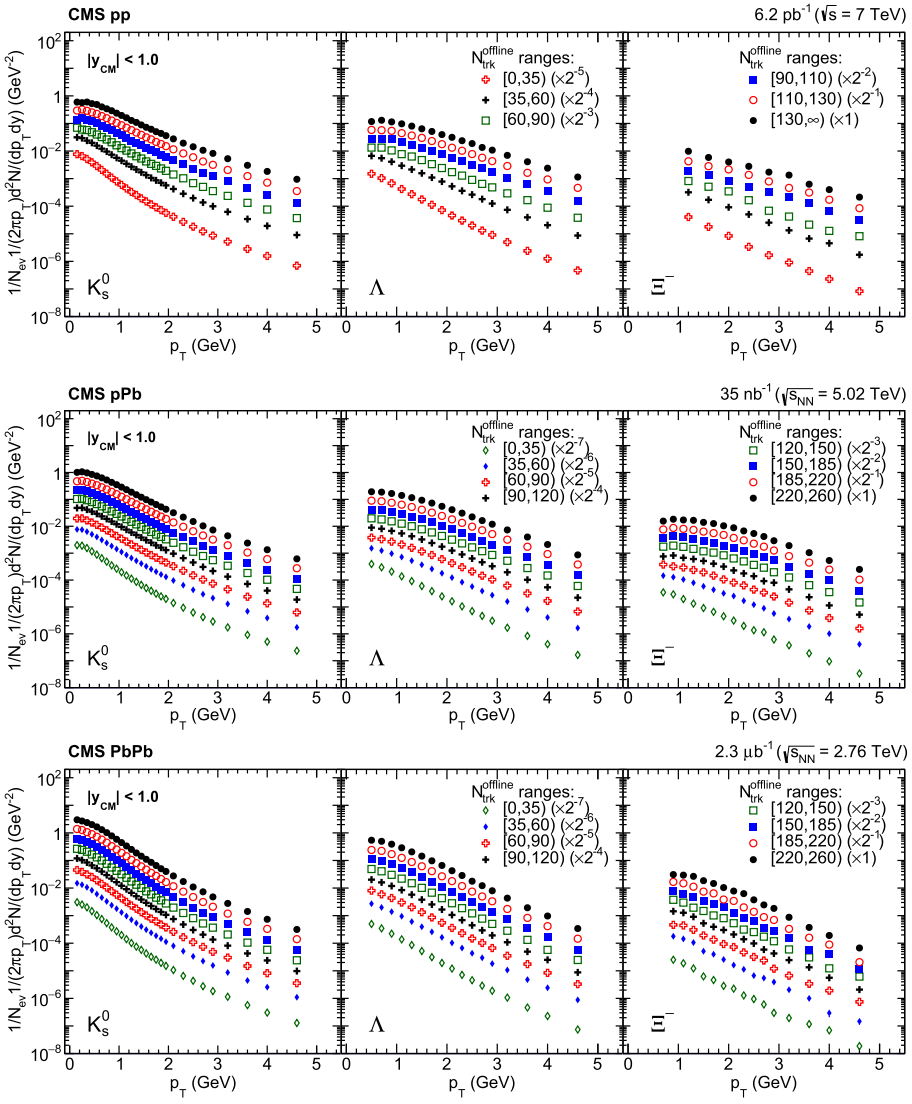

Fig. 2. The p_{T} spectra of $\mathrm{K}^0_{\mathrm{S}}$, Λ, and Ξ^- particles in the center-of-mass rapidity range $|y_{\mathrm{cm}}| < 1$ in pp collisions at $\sqrt{s} = 7\,\mathrm{TeV}$ (top), pPb collisions at $\sqrt{s} = 5.02\,\mathrm{TeV}$ (middle), and PbPb collisions at $\sqrt{s_{NN}} = 2.76\,\mathrm{TeV}$ (bottom) for different multiplicity intervals. The inclusion of the charge-conjugate states is implied for Λ and Ξ^- particles. The data in the different multiplicity intervals are scaled by factors of 2^{-n} for better visibility. The statistical uncertainties are smaller than the markers and the systematic uncertainties are not shown.

and high-multiplicity events is seen to be largest for the pp data. In the hydrodynamic model of Ref. [31], smaller collision systems like pp produce a larger radial-flow effect than larger systems like pPb or PbPb, for similar multiplicities, which could explain this observation. For $p_{\mathrm{T}} > 2\,\mathrm{GeV}$, the baryon enhancement could be explained by recombination models, in which free quarks recombine to form hadrons [53]. In previous studies (e.g., Ref. [54]), it has been shown that the average p_{T} value of various particle species has only a slight center-of-mass energy dependence (10% at high multiplicity). This dependence is not sufficient to explain the differences observed in Fig. 3 between the various systems.

For each multiplicity interval, the $\Lambda/2\mathrm{K}^0_{\mathrm{S}}$ ratio reaches a maximum that has a similar value for all three collision processes, and then decreases at higher p_{T}. The location of the maximum increases with multiplicity from around $p_{\mathrm{T}} = 2$ to 3 GeV.

The results for the Ξ^-/Λ ratio are shown in Fig. 3 (bottom). In this case, the difference between the low- and high-multiplicity events is much smaller than for the $\Lambda/2\mathrm{K}^0_{\mathrm{S}}$ ratio, for all three collisions systems. For all systems, the Ξ^-/Λ ratio increases with p_{T} and reaches a plateau at around $p_{\mathrm{T}} = 3\,\mathrm{GeV}$. Due to the large systematic uncertainty, it is not possible to draw a conclusion with respect to the radial-flow interpretation.

Motivated by the hydrodynamic model, we perform a simultaneous fit of a blast-wave function [32] to the $\mathrm{K}^0_{\mathrm{S}}$ and Λ spectra in Fig. 2. The fits are restricted to low p_{T} because that is the region in which the blast-wave model is valid. The blast-wave model is strictly appropriate only for directly produced particles, while about 1/3 of the $\mathrm{K}^0_{\mathrm{S}}$ mesons may be from higher mass resonances [55]. The Ξ^- particle is not used in the fit as there are not many Ξ^- at low p_{T}. The fits are performed for each collision system separately. The fit ranges are $0.1 < p_{\mathrm{T}} < 1.5\,\mathrm{GeV}$ for the $\mathrm{K}^0_{\mathrm{S}}$ and $0.6 < p_{\mathrm{T}} < 3.0\,\mathrm{GeV}$ for the Λ. The fitted function is:

$$\frac{1}{p_{\mathrm{T}}}\frac{\mathrm{d}N}{\mathrm{d}p_{\mathrm{T}}} \sim \int_0^R r\,\mathrm{d}r\, m_{\mathrm{T}} I_0\left(\frac{p_{\mathrm{T}}\sinh\rho}{T_{\mathrm{kin}}}\right) K_1\left(\frac{m_{\mathrm{T}}\cosh\rho}{T_{\mathrm{kin}}}\right), \tag{3}$$

where $\rho = \tanh^{-1}\beta_{\mathrm{T}} = \tanh^{-1}\left(\beta_{\mathrm{s}}(r/R)^n\right)$ is the velocity profile, R is the radius of the medium (set to unity in the fit), r is the radial distance from the center of the medium in the transverse plane, n is the exponent of the velocity profile, β_{T} is the transverse

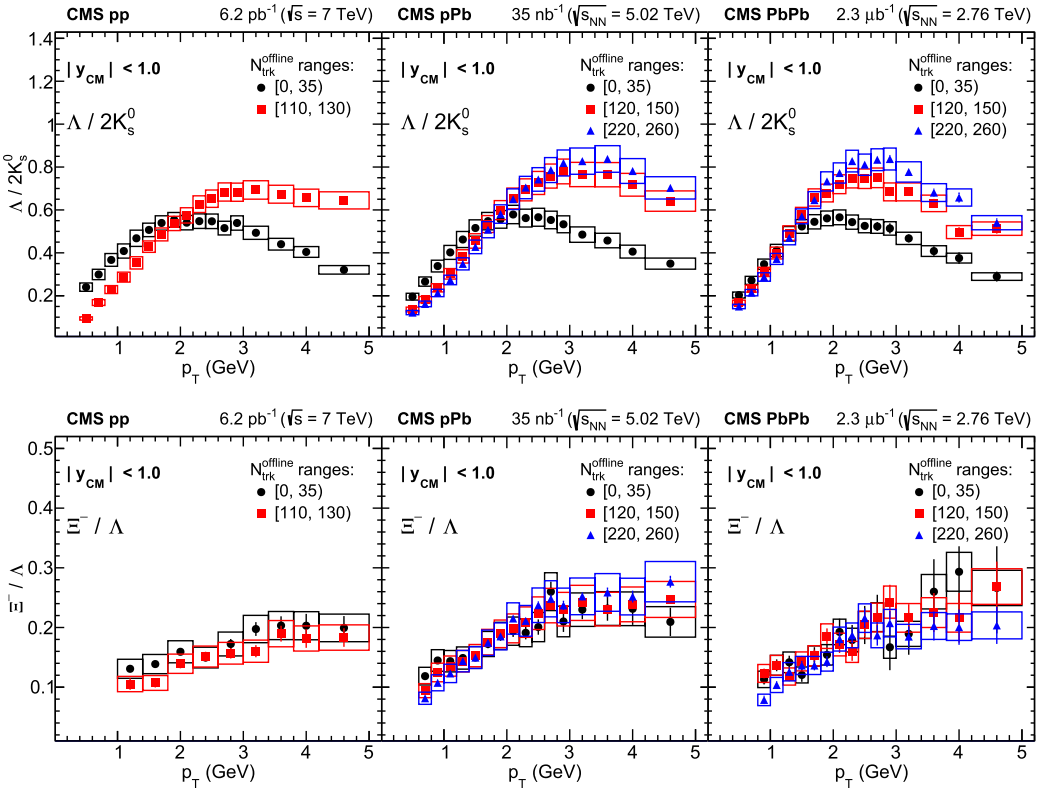

Fig. 3. Ratios of p_T spectra for $\Lambda/2K^0_S$ (top) and Ξ^-/Λ (bottom) in the center-of-mass rapidity range $|y_{cm}| < 1.0$ for pp collisions at $\sqrt{s} = 7\,\text{TeV}$ (left), pPb collisions at $\sqrt{s} = 5.02\,\text{TeV}$ (middle), and PbPb collisions at $\sqrt{s_{NN}} = 2.76\,\text{TeV}$ (right). Two (for pp) or three (for pPb and PbPb) representative multiplicity intervals are presented. The inclusion of the charge-conjugate states is implied for Λ and Ξ^- particles. The error bars represent the statistical uncertainties, while the boxes indicate the systematic uncertainties.

expansion velocity (also known as the radial-flow velocity), β_s is the transverse expansion velocity on the surface of the medium, T_{kin} is the kinetic freeze-out temperature, and I_0 and K_1 are modified Bessel functions. The fitted parameters that govern the shape are n, β_s, and T_{kin}.

In the blast-wave model, common values of T_{kin} and average radial-flow velocity $\langle\beta_T\rangle$ are assumed for all particle species, as is expected if the system is locally thermalized and undergoes a radial-flow expansion. It is useful to directly compare the extracted values of T_{kin} and $\langle\beta_T\rangle$ from the different systems to study the system-size dependence at similar multiplicities.

The extracted values of T_{kin} and $\langle\beta_T\rangle$ are shown in Fig. 4 for the six pp and for the eight pPb and PbPb multiplicity intervals. In this figure, the multiplicity increases from left to right. The ellipses correspond to one standard deviation statistical uncertainties, which for pp collisions are smaller at low and high multiplicity due to the use of events collected with minimum bias and high-multiplicity triggers. Systematic uncertainties, which are evaluated by propagating the systematic uncertainties from the spectra to the blast-wave fits and altering the fit ranges, are on the order of a few percent and are not shown. Examples of the fits are shown in Fig. 5 for a low- and high-multiplicity range in pPb collisions. In general, the fit quality is good for high-multiplicity events except for the lowest p_T range, while for low-multiplicity events there are discrepancies on the order of 5%. However, the discrepancies between the fit and data lie within the systematic uncertainty.

The precise meaning of the T_{kin} and $\langle\beta_T\rangle$ parameters is model dependent, and they should not be interpreted literally as the kinetic freeze-out temperature and radial-flow velocity of the system. The main purpose of Fig. 4 is to provide a qualitative comparison of the spectral shapes in the three systems. In the context

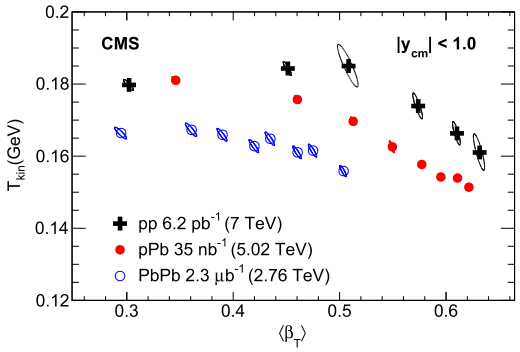

Fig. 4. The extracted kinetic freeze-out temperature, T_{kin}, versus the average radial-flow velocity, $\langle\beta_T\rangle$, from a simultaneous blast-wave fit to the K^0_S and Λ p_T spectra at $|y_{cm}| < 1$ for different multiplicity intervals in pp, pPb, and PbPb collisions. The six pp and eight pPb and PbPb multiplicity intervals are indicated in the legend of Fig. 2. For the results in this plot, the multiplicity increases from left to right. The correlation ellipses represent the statistical uncertainties. Systematic uncertainties, which are evaluated to be on the order of a few percent, are not shown.

of the blast-wave model, when comparing at similar multiplicities, the T_{kin} parameter has the same value within 15% among the three systems, while the $\langle\beta_T\rangle$ parameter is larger when the system is smaller, i.e., $\langle\beta_T\rangle_{pp} > \langle\beta_T\rangle_{pPb} > \langle\beta_T\rangle_{PbPb}$. This is qualitatively consistent with the prediction of Ref. [31]. The results of blast-wave fits are known to depend on the particle species. Due to the limited set of particles in this analysis, future studies will be needed to further substantiate the conclusions.

The evolution of the p_T spectra with multiplicity can be compared more directly between the three systems through examination of the $\langle KE_T\rangle$ value. The $\langle KE_T\rangle$ values at $|y_{cm}| < 1$ for K^0_S, Λ,

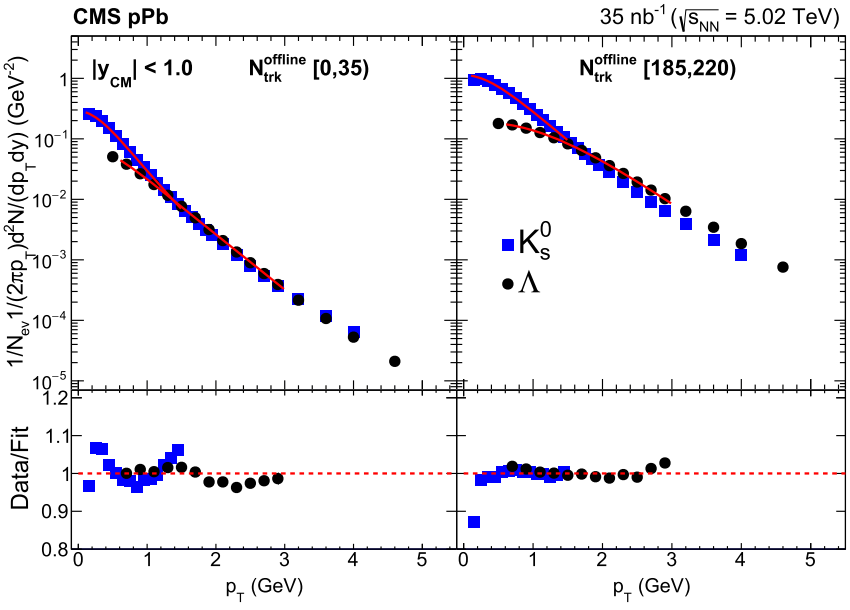

Fig. 5. Examples of simultaneous blast-wave fits of the p_T spectra of K_S^0 and Λ particles in low- and high-multiplicity pPb events. The inclusion of the charge-conjugate states is implied for Λ particles. The ratios of the fits to the data as a function of p_T are shown in the bottom panels. The uncertainties are statistical only and are too small to be visible for most of the points.

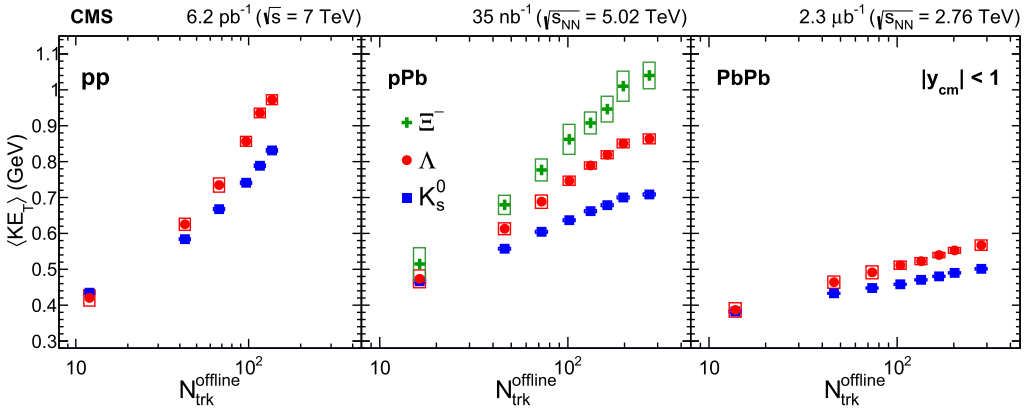

Fig. 6. The average transverse kinetic energy, $\langle KE_T \rangle$, at $|y_{cm}| < 1$ for K_S^0, Λ, and Ξ^- particles as a function of multiplicity in pp, pPb, and PbPb collisions. The inclusion of the charge-conjugate states is implied for Λ and Ξ^- particles. For the Ξ^-, only results from pPb collisions are shown. The error bars represent the statistical uncertainties, while the boxes indicate the systematic uncertainties.

and Ξ^- particles as a function of multiplicity are shown in Fig. 6. Extrapolation of the p_T spectra down to $p_T = 0$ GeV is a crucial step in extracting the $\langle KE_T \rangle$ values, while the impact of the extrapolation up to $p_T \approx \infty$ is negligible, both on the value of $\langle KE_T \rangle$ and its uncertainty. For the Ξ^- particle, only results in pPb collisions are shown due to the limitation of the low-p_T reach in pp and PbPb collisions, as can be seen from Fig. 2. Blast-wave fits to the individual spectra, which only consider the spectrum shape but do not impose any physics constraint, are used to obtain the extrapolation. The fraction of the extrapolated yield with respect to the total yield is about 1.2–2.5% for the K_S^0, 5.8–15.1% for the Λ, and 5.4–20.4% for the Ξ^- particles, depending on the multiplicity. Alternative methods to perform the extrapolation are used to evaluate a systematic uncertainty, including use of the predictions from the simultaneous blast-wave fit to the K_S^0 and Λ p_T spectra, and a linear extrapolation from the yields in a low range of p_T. The systematic uncertainties from Table 2 are also included in the evaluation of the $\langle KE_T \rangle$ uncertainties.

For the lowest multiplicity range, the $\langle KE_T \rangle$ values for each particle species are seen to be similar. For all particle species, $\langle KE_T \rangle$ increases with increasing multiplicity. However, the slope of the increase differs for different particles, with the heavier particles exhibiting a faster growth in $\langle KE_T \rangle$ for all systems. For a given multiplicity range, the $\langle KE_T \rangle$ value is roughly proportional to the particle's mass. In PbPb collisions, this can be understood to be due to the onset of radial flow [2,7]. The observed difference between particle species at high multiplicity is seen to be larger for pp and pPb events than for PbPb events. Note, however, the difference in the center-of-mass energies between the three systems.

6.2. Rapidity dependence in pPb events

The rapidity dependence of the p_T spectra of the K_S^0 and Λ particles is studied in the pPb data. No results for Ξ^- particles are presented due to statistical limitations. As a pPb collision is asymmetric in rapidity, it is interesting to compare the spectra along the Pb-going ($y_{cm} < 0$) and p-going ($y_{cm} > 0$) directions [37]. The

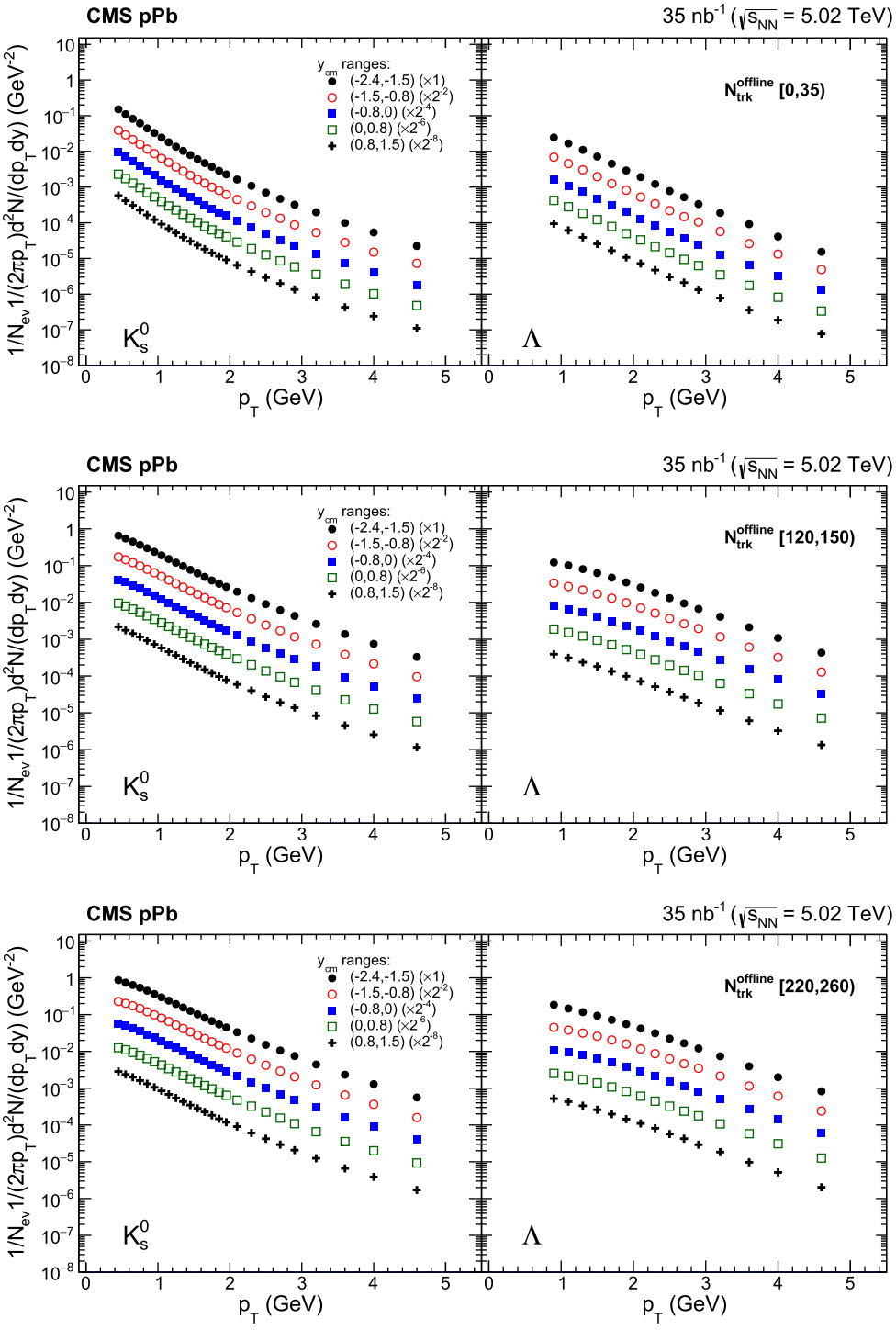

Fig. 7. The p_T spectra of K_S^0 and Λ particles in different y_{cm} ranges for pPb collisions at $\sqrt{s} = 5.02$ TeV. The inclusion of the charge-conjugate states is implied for Λ and particles. Results are shown for three multiplicity ranges: $0 \le N_{trk}^{offline} < 35$ (top), $120 \le N_{trk}^{offline} < 150$ (middle), and $220 \le N_{trk}^{offline} < 260$ (bottom). Within each panel, the curves on top represent Pb-going events and the curves on bottom p-going events. The data in the different rapidity intervals are scaled by factors of 2^{-2n} for better visibility. The statistical uncertainties are smaller than the markers and the systematic uncertainties are not shown.

p_T spectra of K_S^0 and Λ particles in different y_{cm} ranges are shown in Fig. 7 for small (top), intermediate (middle), and large (bottom) average multiplicities.

The $\Lambda/2K_S^0$ ratios from the $-1.5 < y_{cm} < -0.8$ (Pb-going) and $0.8 < y_{cm} < 1.5$ (p-going) rapidity regions are compared in Fig. 8 for multiplicity ranges $0 \le N_{trk}^{offline} < 35$ and $220 \le N_{trk}^{offline} < 260$. For both the low-multiplicity and the high-multiplicity events, the $\Lambda/2K_S^0$ ratio from the Pb-going direction lies above the results from the p-going direction, with the largest difference observed at high p_T in the high-multiplicity sample.

As a further study, we calculate $\langle KE_T \rangle$, following the procedure outlined in Section 6.1, and examine its dependence on y_{cm} for K_S^0 and Λ particles in the pPb collisions. The results are shown in Fig. 9. Although the systematic uncertainties at forward rapidities

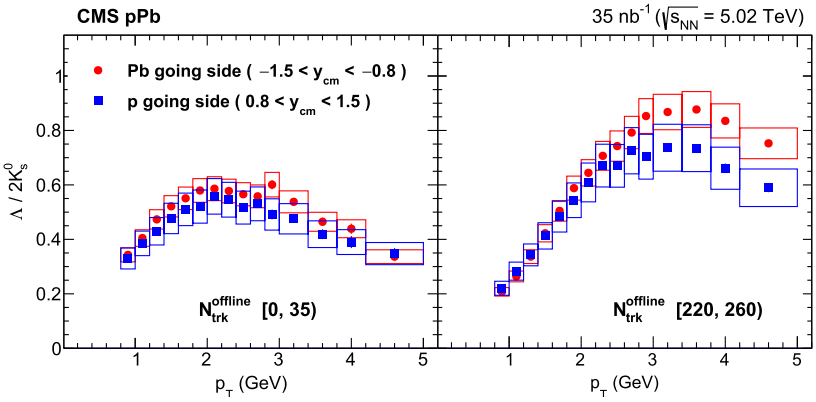

Fig. 8. Ratios of p_T spectra, $\Lambda/2K^0_S$, from the $-1.5 < y_{cm} < -0.8$ (Pb-going) and $0.8 < y_{cm} < 1.5$ (p-going) rapidity regions in pPb collisions at $\sqrt{s} = 5.02$ TeV. The inclusion of the charge-conjugate states is implied for Λ particles. Results are presented for two multiplicity ranges $0 \leq N^{offline}_{trk} < 35$ (left) and $220 \leq N^{offline}_{trk} < 260$ (right). The error bars represent the statistical uncertainties, while the boxes indicate the systematic uncertainties.

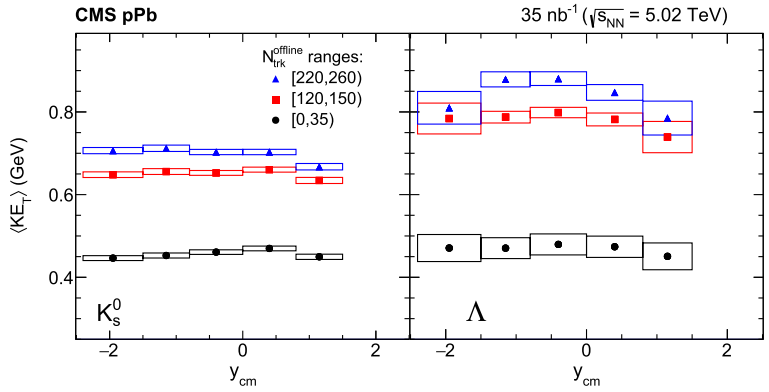

Fig. 9. The average transverse kinetic energy, $\langle KE_T \rangle$, as a function of y_{cm} for the K^0_S and Λ particles in three ranges of multiplicity in pPb collisions at $\sqrt{s} = 5.02$ TeV. The inclusion of the charge-conjugate states is implied for Λ particles. The error bars represent the statistical uncertainties, while the boxes indicate the systematic uncertainties.

are large, the $\langle KE_T \rangle$ values are seen to become slightly asymmetric as multiplicity increases. At low multiplicities ($0 \leq N^{offline}_{trk} < 35$), the ratios of $\langle KE_T \rangle$ between the Pb-going side ($-1.5 < y_{cm} < -0.8$) and the p-going side ($0.8 < y_{cm} < 1.5$) are 1.01 ± 0.01 (syst.) for K^0_S particles and 1.04 ± 0.05 (syst.) for Λ particles, both of which are consistent with unity within the systematic uncertainties (the statistical uncertainties are negligible). However, in the highest multiplicity range, $220 \leq N^{offline}_{trk} < 260$, the ratios become 1.06 ± 0.01 (syst.) for K^0_S particles and 1.12 ± 0.06 (syst.) for Λ particles, suggesting that an asymmetry in $\langle KE_T \rangle$ is developed between the Pb-going and p-going sides. This trend is qualitatively consistent with the hydrodynamic prediction for pPb collisions [37].

7. Summary

Measurements of strange hadron (K^0_S, $\Lambda+\overline{\Lambda}$, and $\Xi^-+\overline{\Xi}^+$) transverse momentum spectra in pp, pPb, and PbPb collisions are presented over a wide range of event charged-particle multiplicity and particle rapidity. The study is based on samples of pp collisions at $\sqrt{s} = 7$ TeV, pPb collisions at $\sqrt{s} = 5.02$ TeV, and PbPb collisions at $\sqrt{s_{NN}} = 2.76$ TeV, collected with the CMS detector at the LHC. In the context of hydrodynamic models, the measured particle spectra are fitted with a blast wave function, which describes an expanding fluid-like system. When comparing at a similar multiplicity, the extracted radial-flow velocity parameters are found to be larger in pp and pPb collisions than that in PbPb collisions. The average transverse kinetic energy $\langle KE_T \rangle$ of strange hadrons is observed to increase with multiplicity, with a stronger increase for heavier particles. At similar multiplicities, the difference in $\langle KE_T \rangle$ between the strange-particle species is larger in the smaller pp and pPb systems than in the PbPb system. For pPb collisions, $\langle KE_T \rangle$ in the Pb-going direction for K^0_S ($\Lambda+\overline{\Lambda}$) is 6% (12%) larger than in the p-going direction for events with the highest particle multiplicities.

Acknowledgements

We congratulate our colleagues in the CERN accelerator departments for the excellent performance of the LHC and thank the technical and administrative staffs at CERN and at other CMS institutes for their contributions to the success of the CMS effort. In addition, we gratefully acknowledge the computing centers and personnel of the Worldwide LHC Computing Grid for delivering so effectively the computing infrastructure essential to our analyses. Finally, we acknowledge the enduring support for the construction and operation of the LHC and the CMS detector provided by the following funding agencies: BMWFW and FWF (Austria); FNRS and FWO (Belgium); CNPq, CAPES, FAPERJ, and FAPESP (Brazil); MES (Bulgaria); CERN; CAS, MoST, and NSFC (China); COLCIENCIAS (Colombia); MSES and CSF (Croatia); RPF (Cyprus); MoER, ERC IUT and ERDF (Estonia); Academy of Finland, MEC, and HIP (Finland); CEA and CNRS/IN2P3 (France); BMBF, DFG, and HGF (Germany); GSRT (Greece); OTKA and NIH (Hungary); DAE and DST (India); IPM (Iran); SFI (Ireland); INFN (Italy); MSIP and NRF (Republic of Korea); LAS (Lithuania); MOE and UM (Malaysia); BUAP, CINVESTAV, CONACYT, LNS, SEP, and UASLP-FAI (Mexico); MBIE (New Zealand); PAEC (Pakistan); MSHE and NSC (Poland); FCT (Portugal); JINR (Dubna); MON, RosAtom, RAS and RFBR (Russia);

MESTD (Serbia); SEIDI and CPAN (Spain); Swiss Funding Agencies (Switzerland); MST (Taipei); ThEPCenter, IPST, STAR and NSTDA (Thailand); TUBITAK and TAEK (Turkey); NASU and SFFR (Ukraine); STFC (United Kingdom); DOE and NSF (USA).

Individuals have received support from the Marie-Curie program and the European Research Council and EPLANET (European Union); the Leventis Foundation; the A.P. Sloan Foundation; the Alexander von Humboldt Foundation; the Belgian Federal Science Policy Office; the Fonds pour la Formation à la Recherche dans l'Industrie et dans l'Agriculture (FRIA-Belgium); the Agentschap voor Innovatie door Wetenschap en Technologie (IWT-Belgium); the Ministry of Education, Youth and Sports (MEYS) of the Czech Republic; the Council of Science and Industrial Research, India; the HOMING PLUS program of the Foundation for Polish Science, cofinanced from European Union, Regional Development Fund; the Mobility Plus program of the Ministry of Science and Higher Education (Poland); the OPUS program of the National Science Center (Poland); the Thalis and Aristeia programs cofinanced by EU-ESF and the Greek NSRF; the National Priorities Research Program by Qatar National Research Fund; the Programa Clarín-COFUND del Principado de Asturias; the Rachadapisek Sompot Fund for Postdoctoral Fellowship, Chulalongkorn University (Thailand); the Chulalongkorn Academic into Its 2nd Century Project Advancement Project (Thailand); and the Welch Foundation, contract C-1845.

References

[1] E. Andersen, et al., Enhancement of central Λ, Ξ and Ω yields in Pb–Pb collisions at 158 A GeV/c, Phys. Lett. B 433 (1998) 209, http://dx.doi.org/10.1016/S0370-2693(98)00689-3.

[2] J. Adams, et al., STAR, Experimental and theoretical challenges in the search for the quark gluon plasma: The STAR Collaboration's critical assessment of the evidence from RHIC collisions, Nucl. Phys. A 757 (2005) 102, http://dx.doi.org/10.1016/j.nuclphysa.2005.03.085, arXiv:nucl-ex/0501009.

[3] J. Rafelski, B. Muller, Strangeness production in the quark–gluon plasma, Phys. Rev. Lett. 48 (1982) 1066, http://dx.doi.org/10.1103/PhysRevLett.48.1066.

[4] B.I. Abelev, et al., STAR, Enhanced strange baryon production in Au + Au collisions compared to $p+p$ at $\sqrt{s_{NN}} = 200$ GeV, Phys. Rev. C 77 (2008) 044908, http://dx.doi.org/10.1103/PhysRevC.77.044908, arXiv:0705.2511.

[5] E. Andersen, et al., WA97, Strangeness enhancement at mid-rapidity in Pb Pb collisions at 158-A-GeV/c, Phys. Lett. B 449 (1999) 401, http://dx.doi.org/10.1016/S0370-2693(99)00140-9.

[6] J. Adams, et al., STAR, Multistrange baryon production in Au–Au collisions at $\sqrt{s_{NN}} = 130$ GeV, Phys. Rev. Lett. 92 (2004) 182301, http://dx.doi.org/10.1103/PhysRevLett.92.182301, arXiv:nucl-ex/0307024.

[7] K. Adcox, et al., PHENIX, Formation of dense partonic matter in relativistic nucleus–nucleus collisions at RHIC: experimental evaluation by the PHENIX Collaboration, Nucl. Phys. A 757 (2005) 184, http://dx.doi.org/10.1016/j.nuclphysa.2005.03.086, arXiv:nucl-ex/0410003.

[8] CMS Collaboration, Observation of long-range near-side angular correlations in proton–proton collisions at the LHC, J. High Energy Phys. 09 (2010) 091, http://dx.doi.org/10.1007/JHEP09(2010)091, arXiv:1009.4122.

[9] CMS Collaboration, Observation of long-range, near-side angular correlations in pPb collisions at the LHC, Phys. Lett. B 718 (2013) 795, http://dx.doi.org/10.1016/j.physletb.2012.11.025, arXiv:1210.5482.

[10] ATLAS Collaboration, Observation of associated near-side and away-side long-range correlations in $\sqrt{s_{NN}} = 5.02$ TeV proton–lead collisions with the ATLAS detector, Phys. Rev. Lett. 110 (2013) 182302, http://dx.doi.org/10.1103/PhysRevLett.110.182302, arXiv:1212.5198.

[11] ALICE Collaboration, Long-range angular correlations on the near and away side in pPb collisions at $\sqrt{s_{NN}} = 5.02$ TeV, Phys. Lett. B 719 (2013) 29, http://dx.doi.org/10.1016/j.physletb.2013.01.012, arXiv:1212.2001.

[12] K. Dusling, W. Li, B. Schenke, Novel collective phenomena in high-energy proton–proton and proton–nucleus collisions, Int. J. Mod. Phys. E 25 (2016) 1630002, http://dx.doi.org/10.1142/S0218301316300022, arXiv:1509.07939.

[13] P. Bożek, Collective flow in p–Pb and d–Pb collisions at TeV energies, Phys. Rev. C 85 (2012) 014911, http://dx.doi.org/10.1103/PhysRevC.85.014911, arXiv:1112.0915.

[14] P. Bożek, W. Broniowski, Correlations from hydrodynamic flow in pPb collisions, Phys. Lett. B 718 (2013) 1557, http://dx.doi.org/10.1016/j.physletb.2012.12.051, arXiv:1211.0845.

[15] A. Bzdak, B. Schenke, P. Tribedy, R. Venugopalan, Initial state geometry and the role of hydrodynamics in proton–proton, proton–nucleus and deuteron–nucleus collisions, Phys. Rev. C 87 (2013) 064906, http://dx.doi.org/10.1103/PhysRevC.87.064906, arXiv:1304.3403.

[16] K. Werner, I. Karpenko, T. Pierog, "Ridge" in proton–proton scattering at 7 TeV, Phys. Rev. Lett. 106 (2011) 122004, http://dx.doi.org/10.1103/PhysRevLett.106.122004, arXiv:1011.0375.

[17] K. Dusling, R. Venugopalan, Explanation of systematics of CMS p+Pb high multiplicity di-hadron data at $\sqrt{s_{NN}} = 5.02$ TeV, Phys. Rev. D 87 (2013) 054014, http://dx.doi.org/10.1103/PhysRevD.87.054014, arXiv:1211.3701.

[18] K. Dusling, R. Venugopalan, Evidence for BFKL and saturation dynamics from dihadron spectra at the LHC, Phys. Rev. D 87 (2013) 051502, http://dx.doi.org/10.1103/PhysRevD.87.051502, arXiv:1210.3890.

[19] A. Dumitru, L. McLerran, V. Skokov, Azimuthal asymmetries and the emergence of "collectivity" from multi-particle correlations in high-energy pA collisions, Phys. Lett. B 743 (2015) 134, http://dx.doi.org/10.1016/j.physletb.2015.02.046, arXiv:1410.4844.

[20] M. Gyulassy, P. Levai, I. Vitev, T.S. Biro, Non-Abelian bremsstrahlung and azimuthal asymmetries in high energy $p+A$ reactions, Phys. Rev. D 90 (2014) 054025, http://dx.doi.org/10.1103/PhysRevD.90.054025, arXiv:1405.7825.

[21] W. Li, Observation of a 'ridge' correlation structure in high multiplicity proton–proton collisions: a brief review, Mod. Phys. Lett. A 27 (2012) 1230018, http://dx.doi.org/10.1142/S0217732312300182, arXiv:1206.0148.

[22] L. He, T. Edmonds, Z.-W. Lin, F. Liu, D. Molnar, F. Wang, Anisotropic parton escape is the dominant source of azimuthal anisotropy in transport models, Phys. Lett. B 753 (2016) 506, http://dx.doi.org/10.1016/j.physletb.2015.12.051, arXiv:1502.05572.

[23] ALICE Collaboration, Centrality dependence of π, K, p production in Pb–Pb collisions at $\sqrt{s_{NN}} = 2.76$ TeV, Phys. Rev. C 88 (2013) 044910, http://dx.doi.org/10.1103/PhysRevC.88.044910, arXiv:1303.0737.

[24] ALICE Collaboration, Elliptic flow of identified hadrons in Pb–Pb collisions at $\sqrt{s_{NN}} = 2.76$ TeV, J. High Energy Phys. 06 (2015) 190, http://dx.doi.org/10.1007/JHEP06(2015)190, arXiv:1405.4632.

[25] H. Song, S. Bass, U.W. Heinz, Spectra and elliptic flow for identified hadrons in 2.76A TeV Pb+Pb collisions, Phys. Rev. C 89 (2014) 034919, http://dx.doi.org/10.1103/PhysRevC.89.034919, arXiv:1311.0157.

[26] X. Zhu, F. Meng, H. Song, Y.-X. Liu, Hybrid model approach for strange and multistrange hadrons in 2.76A TeV Pb+Pb collisions, Phys. Rev. C 91 (2015) 034904, http://dx.doi.org/10.1103/PhysRevC.91.034904, arXiv:1501.03286.

[27] ALICE Collaboration, Multiplicity dependence of pion, kaon, proton and lambda production in p–pb collisions at $\sqrt{s_{NN}} = 5.02$ TeV, Phys. Lett. B 728 (2014) 25, http://dx.doi.org/10.1016/j.physletb.2013.11.020, arXiv:1307.6796.

[28] CMS Collaboration, Study of the production of charged pions, kaons, and protons in pPb collisions at $\sqrt{s_{NN}} = 5.02$ TeV, Eur. Phys. J. C 74 (2014) 2847, http://dx.doi.org/10.1140/epjc/s10052-014-2847-x, arXiv:1307.3442.

[29] ALICE Collaboration, Long-range angular correlations of π, K and p in p–Pb collisions at $\sqrt{s_{NN}} = 5.02$ TeV, Phys. Lett. B 726 (2013) 164, http://dx.doi.org/10.1016/j.physletb.2013.08.024, arXiv:1307.3237.

[30] CMS Collaboration, Long-range two-particle correlations of strange hadrons with charged particles in pPb and PbPb collisions at LHC energies, Phys. Lett. B 742 (2015) 200, http://dx.doi.org/10.1016/j.physletb.2015.01.034, arXiv:1409.3392.

[31] E. Shuryak, I. Zahed, High-multiplicity pp and pA collisions: hydrodynamics at its edge, Phys. Rev. C 88 (2013) 044915, http://dx.doi.org/10.1103/PhysRevC.88.044915, arXiv:1301.4470.

[32] E. Schnedermann, J. Sollfrank, U. Heinz, Thermal phenomenology of hadrons from 200 A GeV S+S collisions, Phys. Rev. C 48 (1993) 2462, http://dx.doi.org/10.1103/PhysRevC.48.2462, arXiv:nucl-th/9307020.

[33] C. Albajar, et al., UA1, A study of the general characteristics of proton–antiproton collisions at $\sqrt{s} = 0.2$ TeV to 0.9 TeV, Nucl. Phys. B 335 (1990) 261, http://dx.doi.org/10.1016/0550-3213(90)90493-W.

[34] T. Alexopoulos, et al., Multiplicity dependence of the transverse momentum spectrum for centrally produced hadrons in antiproton–proton collisions at $\sqrt{s} = 1.8$ TeV, Phys. Rev. Lett. 60 (1988) 1622, http://dx.doi.org/10.1103/PhysRevLett.60.1622.

[35] B.I. Abelev, et al., STAR, Systematic measurements of identified particle spectra in pp, $d+$Au and Au + Au collisions from STAR, Phys. Rev. C 79 (2009) 034909, http://dx.doi.org/10.1103/PhysRevC.79.034909, arXiv:0808.2041.

[36] A. Ortiz Velasquez, P. Christiansen, E. Cuautle Flores, I. Maldonado Cervantes, G. Paić, Color reconnection and flowlike patterns in pp collisions, Phys. Rev. Lett. 111 (2013) 042001, http://dx.doi.org/10.1103/PhysRevLett.111.042001, arXiv:1303.6326.

[37] P. Bożek, A. Bzdak, V. Skokov, The rapidity dependence of the average transverse momentum in p+Pb collisions at the LHC: the color glass condensate versus hydrodynamics, Phys. Lett. B 728 (2014) 662, http://dx.doi.org/10.1016/j.physletb.2013.12.034, arXiv:1309.7358.

[38] CMS Collaboration, Description and performance of track and primary-vertex reconstruction with the CMS tracker, J. Instrum. 9 (2014) P10009, http://dx.doi.org/10.1088/1748-0221/9/10/P10009, arXiv:1405.6569.

[39] CMS Collaboration, The CMS experiment at the CERN LHC, J. Instrum. 3 (2008) S08004, http://dx.doi.org/10.1088/1748-0221/3/08/S08004.

[40] S. Agostinelli, et al., Geant4, Geant4—a simulation toolkit, Nucl. Instrum. Methods A 506 (2003) 250, http://dx.doi.org/10.1016/S0168-9002(03)01368-8.
[41] S. Chatrchyan, et al., CMS, Multiplicity and transverse momentum dependence of two- and four-particle correlations in pPb and PbPb collisions, Phys. Lett. B 724 (2013) 213, http://dx.doi.org/10.1016/j.physletb.2013.06.028, arXiv:1305.0609.
[42] CMS Collaboration, Azimuthal anisotropy of charged particles at high transverse momenta in PbPb collisions at $\sqrt{s_{NN}} = 2.76$ TeV, Phys. Rev. Lett. 109 (2012) 022301, http://dx.doi.org/10.1103/PhysRevLett.109.022301, arXiv:1204.1850.
[43] W. Adam, et al., CMS Trigger, Data Acquisition Group, The CMS high level trigger, Eur. Phys. J. C 46 (2006) 605, http://dx.doi.org/10.1140/epjc/s2006-02495-8, arXiv:hep-ex/0512077.
[44] T. Pierog, I. Karpenko, J.M. Katzy, E. Yatsenko, K. Werner, EPOS LHC: test of collective hadronization with data measured at the CERN Large Hadron Collider, Phys. Rev. C 92 (2015) 034906, http://dx.doi.org/10.1103/PhysRevC.92.034906.
[45] M. Gyulassy, X.-N. Wang, HIJING 1.0: a Monte Carlo program for parton and particle production in high-energy hadronic and nuclear collisions, Comput. Phys. Commun. 83 (1994) 307, http://dx.doi.org/10.1016/0010-4655(94)90057-4, arXiv:nucl-th/9502021.
[46] T. Sjöstrand, S. Mrenna, P. Skands, PYTHIA 6.4 physics and manual, J. High Energy Phys. 05 (2006) 026, http://dx.doi.org/10.1088/1126-6708/2006/05/026, arXiv:hep-ph/0603175.
[47] T. Sjöstrand, S. Mrenna, P. Skands, A brief introduction to PYTHIA 8.1, Comput. Phys. Commun. 178 (2008) 852, http://dx.doi.org/10.1016/j.cpc.2008.01.036, arXiv:0710.3820.
[48] CMS Collaboration, Measurement of tracking efficiency, in: CMS Physics Analysis Summary CMS-PAS-TRK-10-002, 2010, http://cdsweb.cern.ch/record/1279139.
[49] CMS Collaboration, Strange particle production in pp collisions at $\sqrt{s} = 0.9$ and 7 TeV, J. High Energy Phys. 05 (2011) 064, http://dx.doi.org/10.1007/JHEP05(2011)064, arXiv:1102.4282.
[50] Particle Data Group, K.A. Olive, et al., Review of Particle Physics, Chin. Phys. C 38 (2014) 090001, http://dx.doi.org/10.1088/1674-1137/38/9/090001.
[51] P. Bożek, I. Wyskiel-Piekarska, Particle spectra in Pb–Pb collisions at $\sqrt{s_{NN}} = 2.76$ TeV, Phys. Rev. C 85 (2012) 064915, http://dx.doi.org/10.1103/PhysRevC.85.064915, arXiv:1203.6513.
[52] I.A. Karpenko, Yu.M. Sinyukov, K. Werner, Uniform description of bulk observables in the hydrokinetic model of $A + A$ collisions at the BNL Relativistic Heavy Ion Collider and the CERN Large Hadron Collider, Phys. Rev. C 87 (2013) 024914, http://dx.doi.org/10.1103/PhysRevC.87.024914, arXiv:1204.5351.
[53] R.J. Fries, V. Greco, P. Sorensen, Coalescence models for hadron formation from quark gluon plasma, Annu. Rev. Nucl. Part. Sci. 58 (2008) 177, http://dx.doi.org/10.1146/annurev.nucl.58.110707.171134, arXiv:0807.4939.
[54] CMS Collaboration, Study of the inclusive production of charged pions, kaons, and protons in pp collisions at $\sqrt{s} = 0.9$, 2.76, and 7 TeV, Eur. Phys. J. C 72 (2012) 2164, http://dx.doi.org/10.1140/epjc/s10052-012-2164-1, arXiv:1207.4724.
[55] ALICE Collaboration, Production of $K^*(892)^0$ and $\phi(1020)$ in p–Pb collisions at $\sqrt{s_{NN}} = 5.02$ TeV, Eur. Phys. J. C 76 (2016) 245, http://dx.doi.org/10.1140/epjc/s10052-016-4088-7, arXiv:1601.07868.

The CMS Collaboration

V. Khachatryan, A.M. Sirunyan, A. Tumasyan

Yerevan Physics Institute, Yerevan, Armenia

W. Adam, E. Asilar, T. Bergauer, J. Brandstetter, E. Brondolin, M. Dragicevic, J. Erö, M. Flechl, M. Friedl, R. Frühwirth [1], V.M. Ghete, C. Hartl, N. Hörmann, J. Hrubec, M. Jeitler [1], A. König, M. Krammer [1], I. Krätschmer, D. Liko, T. Matsushita, I. Mikulec, D. Rabady, N. Rad, B. Rahbaran, H. Rohringer, J. Schieck [1], J. Strauss, W. Treberer-Treberspurg, W. Waltenberger, C.-E. Wulz [1]

Institut für Hochenergiephysik der OeAW, Wien, Austria

V. Mossolov, N. Shumeiko, J. Suarez Gonzalez

National Centre for Particle and High Energy Physics, Minsk, Belarus

S. Alderweireldt, T. Cornelis, E.A. De Wolf, X. Janssen, A. Knutsson, J. Lauwers, S. Luyckx, M. Van De Klundert, H. Van Haevermaet, P. Van Mechelen, N. Van Remortel, A. Van Spilbeeck

Universiteit Antwerpen, Antwerpen, Belgium

S. Abu Zeid, F. Blekman, J. D'Hondt, N. Daci, I. De Bruyn, K. Deroover, N. Heracleous, J. Keaveney, S. Lowette, S. Moortgat, L. Moreels, A. Olbrechts, Q. Python, D. Strom, S. Tavernier, W. Van Doninck, P. Van Mulders, I. Van Parijs

Vrije Universiteit Brussel, Brussel, Belgium

H. Brun, C. Caillol, B. Clerbaux, G. De Lentdecker, G. Fasanella, L. Favart, R. Goldouzian, A. Grebenyuk, G. Karapostoli, T. Lenzi, A. Léonard, T. Maerschalk, A. Marinov, A. Randle-conde, T. Seva, C. Vander Velde, P. Vanlaer, R. Yonamine, F. Zenoni, F. Zhang [2]

Université Libre de Bruxelles, Bruxelles, Belgium

L. Benucci, A. Cimmino, S. Crucy, D. Dobur, A. Fagot, G. Garcia, M. Gul, J. Mccartin, A.A. Ocampo Rios, D. Poyraz, D. Ryckbosch, S. Salva, R. Schöfbeck, M. Sigamani, M. Tytgat, W. Van Driessche, E. Yazgan, N. Zaganidis

Ghent University, Ghent, Belgium

C. Beluffi [3], O. Bondu, S. Brochet, G. Bruno, A. Caudron, L. Ceard, S. De Visscher, C. Delaere, M. Delcourt, L. Forthomme, B. Francois, A. Giammanco, A. Jafari, P. Jez, M. Komm, V. Lemaitre, A. Magitteri, A. Mertens, M. Musich, C. Nuttens, K. Piotrzkowski, L. Quertenmont, M. Selvaggi, M. Vidal Marono, S. Wertz

Université Catholique de Louvain, Louvain-la-Neuve, Belgium

N. Beliy, G.H. Hammad

Université de Mons, Mons, Belgium

W.L. Aldá Júnior, F.L. Alves, G.A. Alves, L. Brito, M. Correa Martins Junior, M. Hamer, C. Hensel, A. Moraes, M.E. Pol, P. Rebello Teles

Centro Brasileiro de Pesquisas Fisicas, Rio de Janeiro, Brazil

E. Belchior Batista Das Chagas, W. Carvalho, J. Chinellato [4], A. Custódio, E.M. Da Costa, D. De Jesus Damiao, C. De Oliveira Martins, S. Fonseca De Souza, L.M. Huertas Guativa, H. Malbouisson, D. Matos Figueiredo, C. Mora Herrera, L. Mundim, H. Nogima, W.L. Prado Da Silva, A. Santoro, A. Sznajder, E.J. Tonelli Manganote [4], A. Vilela Pereira

Universidade do Estado do Rio de Janeiro, Rio de Janeiro, Brazil

S. Ahuja [a], C.A. Bernardes [b], A. De Souza Santos [b], S. Dogra [a], T.R. Fernandez Perez Tomei [a], E.M. Gregores [b], P.G. Mercadante [b], C.S. Moon [a,5], S.F. Novaes [a], Sandra S. Padula [a], D. Romero Abad [b], J.C. Ruiz Vargas

[a] *Universidade Estadual Paulista, São Paulo, Brazil*
[b] *Universidade Federal do ABC, São Paulo, Brazil*

A. Aleksandrov, R. Hadjiiska, P. Iaydjiev, M. Rodozov, S. Stoykova, G. Sultanov, M. Vutova

Institute for Nuclear Research and Nuclear Energy, Sofia, Bulgaria

A. Dimitrov, I. Glushkov, L. Litov, B. Pavlov, P. Petkov

University of Sofia, Sofia, Bulgaria

W. Fang [6]

Beihang University, Beijing, China

M. Ahmad, J.G. Bian, G.M. Chen, H.S. Chen, M. Chen, T. Cheng, R. Du, C.H. Jiang, D. Leggat, R. Plestina [7], F. Romeo, S.M. Shaheen, A. Spiezia, J. Tao, C. Wang, Z. Wang, H. Zhang

Institute of High Energy Physics, Beijing, China

C. Asawatangtrakuldee, Y. Ban, Q. Li, S. Liu, Y. Mao, S.J. Qian, D. Wang, Z. Xu

State Key Laboratory of Nuclear Physics and Technology, Peking University, Beijing, China

C. Avila, A. Cabrera, L.F. Chaparro Sierra, C. Florez, J.P. Gomez, B. Gomez Moreno, J.C. Sanabria

Universidad de Los Andes, Bogota, Colombia

N. Godinovic, D. Lelas, I. Puljak, P.M. Ribeiro Cipriano

University of Split, Faculty of Electrical Engineering, Mechanical Engineering and Naval Architecture, Split, Croatia

Z. Antunovic, M. Kovac

University of Split, Faculty of Science, Split, Croatia

V. Brigljevic, D. Ferencek, K. Kadija, J. Luetic, S. Micanovic, L. Sudic

Institute Rudjer Boskovic, Zagreb, Croatia

A. Attikis, G. Mavromanolakis, J. Mousa, C. Nicolaou, F. Ptochos, P.A. Razis, H. Rykaczewski

University of Cyprus, Nicosia, Cyprus

M. Finger [8], M. Finger Jr. [8]

Charles University, Prague, Czechia

E. Carrera Jarrin

Universidad San Francisco de Quito, Quito, Ecuador

Y. Assran [9,10], T. Elkafrawy [11], A. Ellithi Kamel [12], A. Mahrous [13]

Academy of Scientific Research and Technology of the Arab Republic of Egypt, Egyptian Network of High Energy Physics, Cairo, Egypt

B. Calpas, M. Kadastik, M. Murumaa, L. Perrini, M. Raidal, A. Tiko, C. Veelken

National Institute of Chemical Physics and Biophysics, Tallinn, Estonia

P. Eerola, J. Pekkanen, M. Voutilainen

Department of Physics, University of Helsinki, Helsinki, Finland

J. Härkönen, V. Karimäki, R. Kinnunen, T. Lampén, K. Lassila-Perini, S. Lehti, T. Lindén, P. Luukka, T. Peltola, J. Tuominiemi, E. Tuovinen, L. Wendland

Helsinki Institute of Physics, Helsinki, Finland

J. Talvitie, T. Tuuva

Lappeenranta University of Technology, Lappeenranta, Finland

M. Besancon, F. Couderc, M. Dejardin, D. Denegri, B. Fabbro, J.L. Faure, C. Favaro, F. Ferri, S. Ganjour, A. Givernaud, P. Gras, G. Hamel de Monchenault, P. Jarry, E. Locci, M. Machet, J. Malcles, J. Rander, A. Rosowsky, M. Titov, A. Zghiche

DSM/IRFU, CEA/Saclay, Gif-sur-Yvette, France

A. Abdulsalam, I. Antropov, S. Baffioni, F. Beaudette, P. Busson, L. Cadamuro, E. Chapon, C. Charlot, O. Davignon, L. Dobrzynski, R. Granier de Cassagnac, M. Jo, S. Lisniak, P. Miné, I.N. Naranjo, M. Nguyen, C. Ochando, G. Ortona, P. Paganini, P. Pigard, S. Regnard, R. Salerno, Y. Sirois, T. Strebler, Y. Yilmaz, A. Zabi

Laboratoire Leprince-Ringuet, Ecole Polytechnique, IN2P3-CNRS, Palaiseau, France

J.-L. Agram [14], J. Andrea, A. Aubin, D. Bloch, J.-M. Brom, M. Buttignol, E.C. Chabert, N. Chanon, C. Collard, E. Conte [14], X. Coubez, J.-C. Fontaine [14], D. Gelé, U. Goerlach, C. Goetzmann, A.-C. Le Bihan, J.A. Merlin [15], K. Skovpen, P. Van Hove

Institut Pluridisciplinaire Hubert Curien, Université de Strasbourg, Université de Haute Alsace Mulhouse, CNRS/IN2P3, Strasbourg, France

S. Gadrat

Centre de Calcul de l'Institut National de Physique Nucleaire et de Physique des Particules, CNRS/IN2P3, Villeurbanne, France

S. Beauceron, C. Bernet, G. Boudoul, E. Bouvier, C.A. Carrillo Montoya, R. Chierici, D. Contardo, B. Courbon, P. Depasse, H. El Mamouni, J. Fan, J. Fay, S. Gascon, M. Gouzevitch, B. Ille, F. Lagarde, I.B. Laktineh, M. Lethuillier, L. Mirabito, A.L. Pequegnot, S. Perries, A. Popov [16], J.D. Ruiz Alvarez, D. Sabes, V. Sordini, M. Vander Donckt, P. Verdier, S. Viret

Université de Lyon, Université Claude Bernard Lyon 1, CNRS-IN2P3, Institut de Physique Nucléaire de Lyon, Villeurbanne, France

T. Toriashvili [17]

Georgian Technical University, Tbilisi, Georgia

Z. Tsamalaidze [8]

Tbilisi State University, Tbilisi, Georgia

C. Autermann, S. Beranek, L. Feld, A. Heister, M.K. Kiesel, K. Klein, M. Lipinski, A. Ostapchuk, M. Preuten, F. Raupach, S. Schael, C. Schomakers, J.F. Schulte, J. Schulz, T. Verlage, H. Weber, V. Zhukov [16]

RWTH Aachen University, I. Physikalisches Institut, Aachen, Germany

M. Ata, M. Brodski, E. Dietz-Laursonn, D. Duchardt, M. Endres, M. Erdmann, S. Erdweg, T. Esch, R. Fischer, A. Güth, T. Hebbeker, C. Heidemann, K. Hoepfner, S. Knutzen, M. Merschmeyer, A. Meyer, P. Millet, S. Mukherjee, M. Olschewski, K. Padeken, P. Papacz, T. Pook, M. Radziej, H. Reithler, M. Rieger, F. Scheuch, L. Sonnenschein, D. Teyssier, S. Thüer

RWTH Aachen University, III. Physikalisches Institut A, Aachen, Germany

V. Cherepanov, Y. Erdogan, G. Flügge, H. Geenen, M. Geisler, F. Hoehle, B. Kargoll, T. Kress, A. Künsken, J. Lingemann, A. Nehrkorn, A. Nowack, I.M. Nugent, C. Pistone, O. Pooth, A. Stahl [15]

RWTH Aachen University, III. Physikalisches Institut B, Aachen, Germany

M. Aldaya Martin, I. Asin, K. Beernaert, O. Behnke, U. Behrens, K. Borras [18], A. Campbell, P. Connor, C. Contreras-Campana, F. Costanza, C. Diez Pardos, G. Dolinska, S. Dooling, G. Eckerlin, D. Eckstein, T. Eichhorn, E. Gallo [19], J. Garay Garcia, A. Geiser, A. Gizhko, J.M. Grados Luyando, P. Gunnellini, A. Harb, J. Hauk, M. Hempel [20], H. Jung, A. Kalogeropoulos, O. Karacheban [20], M. Kasemann, J. Kieseler, C. Kleinwort, I. Korol, W. Lange, A. Lelek, J. Leonard, K. Lipka, A. Lobanov, W. Lohmann [20], R. Mankel, I.-A. Melzer-Pellmann, A.B. Meyer, G. Mittag, J. Mnich, A. Mussgiller, E. Ntomari, D. Pitzl, R. Placakyte, A. Raspereza, B. Roland, M.Ö. Sahin, P. Saxena, T. Schoerner-Sadenius, C. Seitz, S. Spannagel, N. Stefaniuk, K.D. Trippkewitz, G.P. Van Onsem, R. Walsh, C. Wissing

Deutsches Elektronen-Synchrotron, Hamburg, Germany

V. Blobel, M. Centis Vignali, A.R. Draeger, T. Dreyer, J. Erfle, E. Garutti, K. Goebel, D. Gonzalez, M. Görner, J. Haller, M. Hoffmann, R.S. Höing, A. Junkes, R. Klanner, R. Kogler, N. Kovalchuk, T. Lapsien, T. Lenz, I. Marchesini, D. Marconi, M. Meyer, M. Niedziela, D. Nowatschin, J. Ott, F. Pantaleo [15], T. Peiffer, A. Perieanu, N. Pietsch, J. Poehlsen, C. Sander, C. Scharf, P. Schleper, E. Schlieckau, A. Schmidt, S. Schumann, J. Schwandt, H. Stadie, G. Steinbrück, F.M. Stober, H. Tholen, D. Troendle, E. Usai, L. Vanelderen, A. Vanhoefer, B. Vormwald

University of Hamburg, Hamburg, Germany

C. Barth, C. Baus, J. Berger, C. Böser, E. Butz, T. Chwalek, F. Colombo, W. De Boer, A. Descroix, A. Dierlamm, S. Fink, F. Frensch, R. Friese, M. Giffels, A. Gilbert, D. Haitz, F. Hartmann [15], S.M. Heindl, U. Husemann, I. Katkov [16], A. Kornmayer [15], P. Lobelle Pardo, B. Maier, H. Mildner, M.U. Mozer, T. Müller, Th. Müller, M. Plagge, G. Quast, K. Rabbertz, S. Röcker, F. Roscher, M. Schröder, G. Sieber, H.J. Simonis, R. Ulrich, J. Wagner-Kuhr, S. Wayand, M. Weber, T. Weiler, S. Williamson, C. Wöhrmann, R. Wolf

Institut für Experimentelle Kernphysik, Karlsruhe, Germany

G. Anagnostou, G. Daskalakis, T. Geralis, V.A. Giakoumopoulou, A. Kyriakis, D. Loukas, A. Psallidas, I. Topsis-Giotis

Institute of Nuclear and Particle Physics (INPP), NCSR Demokritos, Aghia Paraskevi, Greece

A. Agapitos, S. Kesisoglou, A. Panagiotou, N. Saoulidou, E. Tziaferi

National and Kapodistrian University of Athens, Athens, Greece

I. Evangelou, G. Flouris, C. Foudas, P. Kokkas, N. Loukas, N. Manthos, I. Papadopoulos, E. Paradas, J. Strologas

University of Ioánnina, Ioánnina, Greece

N. Filipovic

MTA-ELTE Lendület CMS Particle and Nuclear Physics Group, Eötvös Loránd University, Hungary

G. Bencze, C. Hajdu, P. Hidas, D. Horvath [21], F. Sikler, V. Veszpremi, G. Vesztergombi [22], A.J. Zsigmond

Wigner Research Centre for Physics, Budapest, Hungary

N. Beni, S. Czellar, J. Karancsi [23], J. Molnar, Z. Szillasi

Institute of Nuclear Research ATOMKI, Debrecen, Hungary

M. Bartók [22], A. Makovec, P. Raics, Z.L. Trocsanyi, B. Ujvari

University of Debrecen, Debrecen, Hungary

S. Choudhury [24], P. Mal, K. Mandal, A. Nayak, D.K. Sahoo, N. Sahoo, S.K. Swain

National Institute of Science Education and Research, Bhubaneswar, India

S. Bansal, S.B. Beri, V. Bhatnagar, R. Chawla, R. Gupta, U. Bhawandeep, A.K. Kalsi, A. Kaur, M. Kaur, R. Kumar, A. Mehta, M. Mittal, J.B. Singh, G. Walia

Panjab University, Chandigarh, India

Ashok Kumar, A. Bhardwaj, B.C. Choudhary, R.B. Garg, S. Keshri, A. Kumar, S. Malhotra, M. Naimuddin, N. Nishu, K. Ranjan, R. Sharma, V. Sharma

University of Delhi, Delhi, India

R. Bhattacharya, S. Bhattacharya, K. Chatterjee, S. Dey, S. Dutta, S. Ghosh, N. Majumdar, A. Modak, K. Mondal, S. Mukhopadhyay, S. Nandan, A. Purohit, A. Roy, D. Roy, S. Roy Chowdhury, S. Sarkar, M. Sharan

Saha Institute of Nuclear Physics, Kolkata, India

R. Chudasama, D. Dutta, V. Jha, V. Kumar, A.K. Mohanty [15], L.M. Pant, P. Shukla, A. Topkar

Bhabha Atomic Research Centre, Mumbai, India

T. Aziz, S. Banerjee, S. Bhowmik [25], R.M. Chatterjee, R.K. Dewanjee, S. Dugad, S. Ganguly, S. Ghosh, M. Guchait, A. Gurtu [26], Sa. Jain, G. Kole, S. Kumar, B. Mahakud, M. Maity [25], G. Majumder, K. Mazumdar, S. Mitra, G.B. Mohanty, B. Parida, T. Sarkar [25], N. Sur, B. Sutar, N. Wickramage [27]

Tata Institute of Fundamental Research, Mumbai, India

S. Chauhan, S. Dube, A. Kapoor, K. Kothekar, A. Rane, S. Sharma

Indian Institute of Science Education and Research (IISER), Pune, India

H. Bakhshiansohi, H. Behnamian, S.M. Etesami [28], A. Fahim [29], M. Khakzad, M. Mohammadi Najafabadi, M. Naseri, S. Paktinat Mehdiabadi, F. Rezaei Hosseinabadi, B. Safarzadeh [30], M. Zeinali

Institute for Research in Fundamental Sciences (IPM), Tehran, Iran

M. Felcini, M. Grunewald

University College Dublin, Dublin, Ireland

M. Abbrescia [a,b], C. Calabria [a,b], C. Caputo [a,b], A. Colaleo [a], D. Creanza [a,c], L. Cristella [a,b], N. De Filippis [a,c], M. De Palma [a,b], L. Fiore [a], G. Iaselli [a,c], G. Maggi [a,c], M. Maggi [a], G. Miniello [a,b], S. My [a,b], S. Nuzzo [a,b], A. Pompili [a,b], G. Pugliese [a,c], R. Radogna [a,b], A. Ranieri [a], G. Selvaggi [a,b], L. Silvestris [a,15], R. Venditti [a,b]

[a] *INFN Sezione di Bari, Bari, Italy*
[b] *Università di Bari, Bari, Italy*
[c] *Politecnico di Bari, Bari, Italy*

G. Abbiendi [a], C. Battilana, D. Bonacorsi [a,b], S. Braibant-Giacomelli [a,b], L. Brigliadori [a,b], R. Campanini [a,b], P. Capiluppi [a,b], A. Castro [a,b], F.R. Cavallo [a], S.S. Chhibra [a,b], G. Codispoti [a,b], M. Cuffiani [a,b], G.M. Dallavalle [a], F. Fabbri [a], A. Fanfani [a,b], D. Fasanella [a,b], P. Giacomelli [a], C. Grandi [a], L. Guiducci [a,b], S. Marcellini [a], G. Masetti [a], A. Montanari [a], F.L. Navarria [a,b], A. Perrotta [a], A.M. Rossi [a,b], T. Rovelli [a,b], G.P. Siroli [a,b], N. Tosi [a,b,15]

[a] *INFN Sezione di Bologna, Bologna, Italy*
[b] *Università di Bologna, Bologna, Italy*

G. Cappello [b], M. Chiorboli [a,b], S. Costa [a,b], A. Di Mattia [a], F. Giordano [a,b], R. Potenza [a,b], A. Tricomi [a,b], C. Tuve [a,b]

[a] *INFN Sezione di Catania, Catania, Italy*
[b] *Università di Catania, Catania, Italy*

G. Barbagli [a], V. Ciulli [a,b], C. Civinini [a], R. D'Alessandro [a,b], E. Focardi [a,b], V. Gori [a,b], P. Lenzi [a,b], M. Meschini [a], S. Paoletti [a], G. Sguazzoni [a], L. Viliani [a,b,15]

[a] *INFN Sezione di Firenze, Firenze, Italy*
[b] *Università di Firenze, Firenze, Italy*

L. Benussi, S. Bianco, F. Fabbri, D. Piccolo, F. Primavera [15]

INFN Laboratori Nazionali di Frascati, Frascati, Italy

V. Calvelli [a,b], F. Ferro [a], M. Lo Vetere [a,b], M.R. Monge [a,b], E. Robutti [a], S. Tosi [a,b]

[a] *INFN Sezione di Genova, Genova, Italy*
[b] *Università di Genova, Genova, Italy*

L. Brianza, M.E. Dinardo [a,b], S. Fiorendi [a,b], S. Gennai [a], A. Ghezzi [a,b], P. Govoni [a,b], S. Malvezzi [a], R.A. Manzoni [a,b,15], B. Marzocchi [a,b], D. Menasce [a], L. Moroni [a], M. Paganoni [a,b], D. Pedrini [a], S. Pigazzini, S. Ragazzi [a,b], N. Redaelli [a], T. Tabarelli de Fatis [a,b]

[a] *INFN Sezione di Milano-Bicocca, Milano, Italy*
[b] *Università di Milano-Bicocca, Milano, Italy*

S. Buontempo [a], N. Cavallo [a,c], S. Di Guida [a,d,15], M. Esposito [a,b], F. Fabozzi [a,c], A.O.M. Iorio [a,b], G. Lanza [a], L. Lista [a], S. Meola [a,d,15], M. Merola [a], P. Paolucci [a,15], C. Sciacca [a,b], F. Thyssen

[a] *INFN Sezione di Napoli, Napoli, Italy*
[b] *Università di Napoli 'Federico II', Napoli, Italy*
[c] *Università della Basilicata, Potenza, Italy*
[d] *Università G. Marconi, Roma, Italy*

P. Azzi [a,15], N. Bacchetta [a], M. Bellato [a], L. Benato [a,b], A. Boletti [a,b], M. Dall'Osso [a,b], P. De Castro Manzano [a], T. Dorigo [a], F. Fanzago [a], F. Gonella [a], A. Gozzelino [a], S. Lacaprara [a], M. Margoni [a,b], G. Maron [a,31], A.T. Meneguzzo [a,b], F. Montecassiano [a], M. Passaseo [a], J. Pazzini [a,b,15], M. Pegoraro [a], N. Pozzobon [a,b], P. Ronchese [a,b], M. Sgaravatto [a], F. Simonetto [a,b], E. Torassa [a], M. Tosi [a,b], S. Vanini [a,b], S. Ventura [a], M. Zanetti, P. Zotto [a,b], A. Zucchetta [a,b]

[a] *INFN Sezione di Padova, Padova, Italy*
[b] *Università di Padova, Padova, Italy*
[c] *Università di Trento, Trento, Italy*

A. Braghieri [a], A. Magnani [a,b], P. Montagna [a,b], S.P. Ratti [a,b], V. Re [a], C. Riccardi [a,b], P. Salvini [a], I. Vai [a,b], P. Vitulo [a,b]

[a] *INFN Sezione di Pavia, Pavia, Italy*
[b] *Università di Pavia, Pavia, Italy*

L. Alunni Solestizi [a,b], G.M. Bilei [a], D. Ciangottini [a,b], L. Fanò [a,b], P. Lariccia [a,b], R. Leonardi [a,b], G. Mantovani [a,b], M. Menichelli [a], A. Saha [a], A. Santocchia [a,b]

[a] *INFN Sezione di Perugia, Perugia, Italy*
[b] *Università di Perugia, Perugia, Italy*

K. Androsov [a,32], P. Azzurri [a,15], G. Bagliesi [a], J. Bernardini [a], T. Boccali [a], R. Castaldi [a], M.A. Ciocci [a,32], R. Dell'Orso [a], S. Donato [a,c], G. Fedi, A. Giassi [a], M.T. Grippo [a,32], F. Ligabue [a,c], T. Lomtadze [a], L. Martini [a,b], A. Messineo [a,b], F. Palla [a], A. Rizzi [a,b], A. Savoy-Navarro [a,33], P. Spagnolo [a], R. Tenchini [a], G. Tonelli [a,b], A. Venturi [a], P.G. Verdini [a]

[a] *INFN Sezione di Pisa, Pisa, Italy*
[b] *Università di Pisa, Pisa, Italy*
[c] *Scuola Normale Superiore di Pisa, Pisa, Italy*

L. Barone [a,b], F. Cavallari [a], G. D'imperio [a,b,15], D. Del Re [a,b,15], M. Diemoz [a], S. Gelli [a,b], C. Jorda [a], E. Longo [a,b], F. Margaroli [a,b], P. Meridiani [a], G. Organtini [a,b], R. Paramatti [a], F. Preiato [a,b], S. Rahatlou [a,b], C. Rovelli [a], F. Santanastasio [a,b]

[a] *INFN Sezione di Roma, Roma, Italy*
[b] *Università di Roma, Roma, Italy*

N. Amapane [a,b], R. Arcidiacono [a,c,15], S. Argiro [a,b], M. Arneodo [a,c], N. Bartosik [a], R. Bellan [a,b], C. Biino [a], N. Cartiglia [a], M. Costa [a,b], R. Covarelli [a,b], A. Degano [a,b], N. Demaria [a], L. Finco [a,b], B. Kiani [a,b], C. Mariotti [a], S. Maselli [a], E. Migliore [a,b], V. Monaco [a,b], E. Monteil [a,b], M.M. Obertino [a,b], L. Pacher [a,b], N. Pastrone [a], M. Pelliccioni [a], G.L. Pinna Angioni [a,b], F. Ravera [a,b], A. Romero [a,b], M. Ruspa [a,c], R. Sacchi [a,b], V. Sola [a], A. Solano [a,b], A. Staiano [a], P. Traczyk [a,b]

[a] *INFN Sezione di Torino, Torino, Italy*
[b] *Università di Torino, Torino, Italy*
[c] *Università del Piemonte Orientale, Novara, Italy*

S. Belforte [a], V. Candelise [a,b], M. Casarsa [a], F. Cossutti [a], G. Della Ricca [a,b], C. La Licata [a,b], A. Schizzi [a,b], A. Zanetti [a]

[a] *INFN Sezione di Trieste, Trieste, Italy*
[b] *Università di Trieste, Trieste, Italy*

S.K. Nam

Kangwon National University, Chunchon, Republic of Korea

D.H. Kim, G.N. Kim, M.S. Kim, D.J. Kong, S. Lee, S.W. Lee, Y.D. Oh, A. Sakharov, D.C. Son, Y.C. Yang

Kyungpook National University, Daegu, Republic of Korea

J.A. Brochero Cifuentes, H. Kim, T.J. Kim [34]

Chonbuk National University, Jeonju, Republic of Korea

S. Song

Chonnam National University, Institute for Universe and Elementary Particles, Kwangju, Republic of Korea

S. Cho, S. Choi, Y. Go, D. Gyun, B. Hong, Y. Jo, Y. Kim, B. Lee, K. Lee, K.S. Lee, S. Lee, J. Lim, S.K. Park, Y. Roh

Korea University, Seoul, Republic of Korea

H.D. Yoo

Seoul National University, Seoul, Republic of Korea

M. Choi, H. Kim, H. Kim, J.H. Kim, J.S.H. Lee, I.C. Park, G. Ryu, M.S. Ryu

University of Seoul, Seoul, Republic of Korea

Y. Choi, J. Goh, D. Kim, E. Kwon, J. Lee, I. Yu

Sungkyunkwan University, Suwon, Republic of Korea

V. Dudenas, A. Juodagalvis, J. Vaitkus

Vilnius University, Vilnius, Lithuania

I. Ahmed, Z.A. Ibrahim, J.R. Komaragiri, M.A.B. Md Ali [35], F. Mohamad Idris [36], W.A.T. Wan Abdullah, M.N. Yusli, Z. Zolkapli

National Centre for Particle Physics, Universiti Malaya, Kuala Lumpur, Malaysia

E. Casimiro Linares, H. Castilla-Valdez, E. De La Cruz-Burelo, I. Heredia-De La Cruz [37], A. Hernandez-Almada, R. Lopez-Fernandez, J. Mejia Guisao, A. Sanchez-Hernandez

Centro de Investigacion y de Estudios Avanzados del IPN, Mexico City, Mexico

S. Carrillo Moreno, F. Vazquez Valencia

Universidad Iberoamericana, Mexico City, Mexico

I. Pedraza, H.A. Salazar Ibarguen, C. Uribe Estrada

Benemerita Universidad Autonoma de Puebla, Puebla, Mexico

A. Morelos Pineda

Universidad Autónoma de San Luis Potosí, San Luis Potosí, Mexico

D. Krofcheck

University of Auckland, Auckland, New Zealand

P.H. Butler

University of Canterbury, Christchurch, New Zealand

A. Ahmad, M. Ahmad, Q. Hassan, H.R. Hoorani, W.A. Khan, T. Khurshid, M. Shoaib, M. Waqas

National Centre for Physics, Quaid-I-Azam University, Islamabad, Pakistan

H. Bialkowska, M. Bluj, B. Boimska, T. Frueboes, M. Górski, M. Kazana, K. Nawrocki, K. Romanowska-Rybinska, M. Szleper, P. Zalewski

National Centre for Nuclear Research, Swierk, Poland

G. Brona, K. Bunkowski, A. Byszuk [38], K. Doroba, A. Kalinowski, M. Konecki, J. Krolikowski, M. Misiura, M. Olszewski, M. Walczak

Institute of Experimental Physics, Faculty of Physics, University of Warsaw, Warsaw, Poland

P. Bargassa, C. Beirão Da Cruz E Silva, A. Di Francesco, P. Faccioli, P.G. Ferreira Parracho, M. Gallinaro, J. Hollar, N. Leonardo, L. Lloret Iglesias, M.V. Nemallapudi, F. Nguyen, J. Rodrigues Antunes, J. Seixas, O. Toldaiev, D. Vadruccio, J. Varela, P. Vischia

Laboratório de Instrumentação e Física Experimental de Partículas, Lisboa, Portugal

S. Afanasiev, P. Bunin, M. Gavrilenko, I. Golutvin, I. Gorbunov, A. Kamenev, V. Karjavin, A. Lanev, A. Malakhov, V. Matveev [39,40], P. Moisenz, V. Palichik, V. Perelygin, S. Shmatov, S. Shulha, N. Skatchkov, V. Smirnov, N. Voytishin, A. Zarubin

Joint Institute for Nuclear Research, Dubna, Russia

V. Golovtsov, Y. Ivanov, V. Kim [41], E. Kuznetsova [42], P. Levchenko, V. Murzin, V. Oreshkin, I. Smirnov, V. Sulimov, L. Uvarov, S. Vavilov, A. Vorobyev

Petersburg Nuclear Physics Institute, Gatchina (St. Petersburg), Russia

Yu. Andreev, A. Dermenev, S. Gninenko, N. Golubev, A. Karneyeu, M. Kirsanov, N. Krasnikov, A. Pashenkov, D. Tlisov, A. Toropin

Institute for Nuclear Research, Moscow, Russia

V. Epshteyn, V. Gavrilov, N. Lychkovskaya, V. Popov, I. Pozdnyakov, G. Safronov, A. Spiridonov, M. Toms, E. Vlasov, A. Zhokin

Institute for Theoretical and Experimental Physics, Moscow, Russia

M. Chadeeva, O. Markin, E. Popova, V. Rusinov, E. Tarkovskii

National Research Nuclear University 'Moscow Engineering Physics Institute' (MEPhI), Moscow, Russia

V. Andreev, M. Azarkin [40], I. Dremin [40], M. Kirakosyan, A. Leonidov [40], G. Mesyats, S.V. Rusakov

P.N. Lebedev Physical Institute, Moscow, Russia

A. Baskakov, A. Belyaev, E. Boos, A. Ershov, A. Gribushin, V. Klyukhin, O. Kodolova, V. Korotkikh, I. Lokhtin, I. Miagkov, S. Obraztsov, S. Petrushanko, V. Savrin, A. Snigirev, I. Vardanyan

Skobeltsyn Institute of Nuclear Physics, Lomonosov Moscow State University, Moscow, Russia

I. Azhgirey, I. Bayshev, S. Bitioukov, V. Kachanov, A. Kalinin, D. Konstantinov, V. Krychkine, V. Petrov, R. Ryutin, A. Sobol, L. Tourtchanovitch, S. Troshin, N. Tyurin, A. Uzunian, A. Volkov

State Research Center of Russian Federation, Institute for High Energy Physics, Protvino, Russia

P. Adzic [43], P. Cirkovic, D. Devetak, J. Milosevic, V. Rekovic

University of Belgrade, Faculty of Physics and Vinca Institute of Nuclear Sciences, Belgrade, Serbia

J. Alcaraz Maestre, E. Calvo, M. Cerrada, M. Chamizo Llatas, N. Colino, B. De La Cruz, A. Delgado Peris, A. Escalante Del Valle, C. Fernandez Bedoya, J.P. Fernández Ramos, J. Flix, M.C. Fouz, P. Garcia-Abia, O. Gonzalez Lopez, S. Goy Lopez, J.M. Hernandez, M.I. Josa, E. Navarro De Martino, A. Pérez-Calero Yzquierdo, J. Puerta Pelayo, A. Quintario Olmeda, I. Redondo, L. Romero, M.S. Soares

Centro de Investigaciones Energéticas Medioambientales y Tecnológicas (CIEMAT), Madrid, Spain

J.F. de Trocóniz, M. Missiroli, D. Moran

Universidad Autónoma de Madrid, Madrid, Spain

J. Cuevas, J. Fernandez Menendez, S. Folgueras, I. Gonzalez Caballero, E. Palencia Cortezon, J.M. Vizan Garcia

Universidad de Oviedo, Oviedo, Spain

I.J. Cabrillo, A. Calderon, J.R. Castiñeiras De Saa, E. Curras, M. Fernandez, J. Garcia-Ferrero, G. Gomez, A. Lopez Virto, J. Marco, R. Marco, C. Martinez Rivero, F. Matorras, J. Piedra Gomez, T. Rodrigo, A.Y. Rodríguez-Marrero, A. Ruiz-Jimeno, L. Scodellaro, N. Trevisani, I. Vila, R. Vilar Cortabitarte

Instituto de Física de Cantabria (IFCA), CSIC-Universidad de Cantabria, Santander, Spain

D. Abbaneo, E. Auffray, G. Auzinger, M. Bachtis, P. Baillon, A.H. Ball, D. Barney, A. Benaglia, L. Benhabib, G.M. Berruti, P. Bloch, A. Bocci, A. Bonato, C. Botta, H. Breuker, T. Camporesi, R. Castello, M. Cepeda, G. Cerminara, M. D'Alfonso, D. d'Enterria, A. Dabrowski, V. Daponte, A. David, M. De Gruttola, F. De Guio, A. De Roeck, E. Di Marco [44], M. Dobson, M. Dordevic, B. Dorney, T. du Pree, D. Duggan, M. Dünser, N. Dupont, A. Elliott-Peisert, S. Fartoukh, G. Franzoni, J. Fulcher, W. Funk, D. Gigi, K. Gill, M. Girone, F. Glege, R. Guida, S. Gundacker, M. Guthoff, J. Hammer, P. Harris, J. Hegeman, V. Innocente, P. Janot, H. Kirschenmann, V. Knünz, M.J. Kortelainen, K. Kousouris, P. Lecoq, C. Lourenço, M.T. Lucchini, N. Magini, L. Malgeri, M. Mannelli, A. Martelli, L. Masetti, F. Meijers, S. Mersi, E. Meschi, F. Moortgat,

S. Morovic, M. Mulders, H. Neugebauer, S. Orfanelli [45], L. Orsini, L. Pape, E. Perez, M. Peruzzi, A. Petrilli, G. Petrucciani, A. Pfeiffer, M. Pierini, D. Piparo, A. Racz, T. Reis, G. Rolandi [46], M. Rovere, M. Ruan, H. Sakulin, J.B. Sauvan, C. Schäfer, C. Schwick, M. Seidel, A. Sharma, P. Silva, M. Simon, P. Sphicas [47], J. Steggemann, M. Stoye, Y. Takahashi, D. Treille, A. Triossi, A. Tsirou, V. Veckalns [48], G.I. Veres [22], N. Wardle, H.K. Wöhri, A. Zagozdzinska [38], W.D. Zeuner

CERN, European Organization for Nuclear Research, Geneva, Switzerland

W. Bertl, K. Deiters, W. Erdmann, R. Horisberger, Q. Ingram, H.C. Kaestli, D. Kotlinski, U. Langenegger, T. Rohe

Paul Scherrer Institut, Villigen, Switzerland

F. Bachmair, L. Bäni, L. Bianchini, B. Casal, G. Dissertori, M. Dittmar, M. Donegà, P. Eller, C. Grab, C. Heidegger, D. Hits, J. Hoss, G. Kasieczka, P. Lecomte [†], W. Lustermann, B. Mangano, M. Marionneau, P. Martinez Ruiz del Arbol, M. Masciovecchio, M.T. Meinhard, D. Meister, F. Micheli, P. Musella, F. Nessi-Tedaldi, F. Pandolfi, J. Pata, F. Pauss, G. Perrin, L. Perrozzi, M. Quittnat, M. Rossini, M. Schönenberger, A. Starodumov [49], M. Takahashi, V.R. Tavolaro, K. Theofilatos, R. Wallny

Institute for Particle Physics, ETH Zurich, Zurich, Switzerland

T.K. Aarrestad, C. Amsler [50], L. Caminada, M.F. Canelli, V. Chiochia, A. De Cosa, C. Galloni, A. Hinzmann, T. Hreus, B. Kilminster, C. Lange, J. Ngadiuba, D. Pinna, G. Rauco, P. Robmann, D. Salerno, Y. Yang

Universität Zürich, Zurich, Switzerland

K.H. Chen, T.H. Doan, Sh. Jain, R. Khurana, M. Konyushikhin, C.M. Kuo, W. Lin, Y.J. Lu, A. Pozdnyakov, S.S. Yu

National Central University, Chung-Li, Taiwan

Arun Kumar, P. Chang, Y.H. Chang, Y.W. Chang, Y. Chao, K.F. Chen, P.H. Chen, C. Dietz, F. Fiori, W.-S. Hou, Y. Hsiung, Y.F. Liu, R.-S. Lu, M. Miñano Moya, J.f. Tsai, Y.M. Tzeng

National Taiwan University (NTU), Taipei, Taiwan

B. Asavapibhop, K. Kovitanggoon, G. Singh, N. Srimanobhas, N. Suwonjandee

Chulalongkorn University, Faculty of Science, Department of Physics, Bangkok, Thailand

A. Adiguzel, S. Cerci [51], S. Damarseckin, Z.S. Demiroglu, C. Dozen, I. Dumanoglu, S. Girgis, G. Gokbulut, Y. Guler, E. Gurpinar, I. Hos, E.E. Kangal [52], A. Kayis Topaksu, G. Onengut [53], K. Ozdemir [54], A. Polatoz, B. Tali [51], H. Topakli [55], C. Zorbilmez

Cukurova University, Adana, Turkey

B. Bilin, S. Bilmis, B. Isildak [56], G. Karapinar [57], M. Yalvac, M. Zeyrek

Middle East Technical University, Physics Department, Ankara, Turkey

E. Gülmez, M. Kaya [58], O. Kaya [59], E.A. Yetkin [60], T. Yetkin [61]

Bogazici University, Istanbul, Turkey

A. Cakir, K. Cankocak, S. Sen [62], F.I. Vardarlı

Istanbul Technical University, Istanbul, Turkey

B. Grynyov

Institute for Scintillation Materials of National Academy of Science of Ukraine, Kharkov, Ukraine

L. Levchuk, P. Sorokin

National Scientific Center, Kharkov Institute of Physics and Technology, Kharkov, Ukraine

R. Aggleton, F. Ball, L. Beck, J.J. Brooke, D. Burns, E. Clement, D. Cussans, H. Flacher, J. Goldstein, M. Grimes, G.P. Heath, H.F. Heath, J. Jacob, L. Kreczko, C. Lucas, Z. Meng, D.M. Newbold [63], S. Paramesvaran, A. Poll, T. Sakuma, S. Seif El Nasr-storey, S. Senkin, D. Smith, V.J. Smith

University of Bristol, Bristol, United Kingdom

A. Belyaev [64], C. Brew, R.M. Brown, L. Calligaris, D. Cieri, D.J.A. Cockerill, J.A. Coughlan, K. Harder, S. Harper, E. Olaiya, D. Petyt, C.H. Shepherd-Themistocleous, A. Thea, I.R. Tomalin, T. Williams, S.D. Worm

Rutherford Appleton Laboratory, Didcot, United Kingdom

M. Baber, R. Bainbridge, O. Buchmuller, A. Bundock, D. Burton, S. Casasso, M. Citron, D. Colling, L. Corpe, P. Dauncey, G. Davies, A. De Wit, M. Della Negra, P. Dunne, A. Elwood, D. Futyan, Y. Haddad, G. Hall, G. Iles, R. Lane, R. Lucas [63], L. Lyons, A.-M. Magnan, S. Malik, L. Mastrolorenzo, J. Nash, A. Nikitenko [49], J. Pela, B. Penning, M. Pesaresi, D.M. Raymond, A. Richards, A. Rose, C. Seez, A. Tapper, K. Uchida, M. Vazquez Acosta [65], T. Virdee [15], S.C. Zenz

Imperial College, London, United Kingdom

J.E. Cole, P.R. Hobson, A. Khan, P. Kyberd, D. Leslie, I.D. Reid, P. Symonds, L. Teodorescu, M. Turner

Brunel University, Uxbridge, United Kingdom

A. Borzou, K. Call, J. Dittmann, K. Hatakeyama, H. Liu, N. Pastika

Baylor University, Waco, USA

O. Charaf, S.I. Cooper, C. Henderson, P. Rumerio

The University of Alabama, Tuscaloosa, USA

D. Arcaro, A. Avetisyan, T. Bose, D. Gastler, D. Rankin, C. Richardson, J. Rohlf, L. Sulak, D. Zou

Boston University, Boston, USA

J. Alimena, G. Benelli, E. Berry, D. Cutts, A. Ferapontov, A. Garabedian, J. Hakala, U. Heintz, O. Jesus, E. Laird, G. Landsberg, Z. Mao, M. Narain, S. Piperov, S. Sagir, R. Syarif

Brown University, Providence, USA

R. Breedon, G. Breto, M. Calderon De La Barca Sanchez, S. Chauhan, M. Chertok, J. Conway, R. Conway, P.T. Cox, R. Erbacher, C. Flores, G. Funk, M. Gardner, W. Ko, R. Lander, C. Mclean, M. Mulhearn, D. Pellett, J. Pilot, F. Ricci-Tam, S. Shalhout, J. Smith, M. Squires, D. Stolp, M. Tripathi, S. Wilbur, R. Yohay

University of California, Davis, Davis, USA

R. Cousins, P. Everaerts, A. Florent, J. Hauser, M. Ignatenko, D. Saltzberg, E. Takasugi, V. Valuev, M. Weber

University of California, Los Angeles, USA

K. Burt, R. Clare, J. Ellison, J.W. Gary, G. Hanson, J. Heilman, P. Jandir, E. Kennedy, F. Lacroix, O.R. Long, M. Malberti, M. Olmedo Negrete, M.I. Paneva, A. Shrinivas, H. Wei, S. Wimpenny, B.R. Yates

University of California, Riverside, Riverside, USA

J.G. Branson, G.B. Cerati, S. Cittolin, R.T. D'Agnolo, M. Derdzinski, R. Gerosa, A. Holzner, R. Kelley, D. Klein, J. Letts, I. Macneill, D. Olivito, S. Padhi, M. Pieri, M. Sani, V. Sharma, S. Simon, M. Tadel, A. Vartak, S. Wasserbaech [66], C. Welke, J. Wood, F. Würthwein, A. Yagil, G. Zevi Della Porta

University of California, San Diego, La Jolla, USA

J. Bradmiller-Feld, C. Campagnari, A. Dishaw, V. Dutta, K. Flowers, M. Franco Sevilla, P. Geffert, C. George, F. Golf, L. Gouskos, J. Gran, J. Incandela, N. Mccoll, S.D. Mullin, J. Richman, D. Stuart, I. Suarez, C. West, J. Yoo

University of California, Santa Barbara, Santa Barbara, USA

D. Anderson, A. Apresyan, J. Bendavid, A. Bornheim, J. Bunn, Y. Chen, J. Duarte, A. Mott, H.B. Newman, C. Pena, M. Spiropulu, J.R. Vlimant, S. Xie, R.Y. Zhu

California Institute of Technology, Pasadena, USA

M.B. Andrews, V. Azzolini, A. Calamba, B. Carlson, T. Ferguson, M. Paulini, J. Russ, M. Sun, H. Vogel, I. Vorobiev

Carnegie Mellon University, Pittsburgh, USA

J.P. Cumalat, W.T. Ford, F. Jensen, A. Johnson, M. Krohn, T. Mulholland, K. Stenson, S.R. Wagner

University of Colorado Boulder, Boulder, USA

J. Alexander, A. Chatterjee, J. Chaves, J. Chu, S. Dittmer, N. Eggert, N. Mirman, G. Nicolas Kaufman, J.R. Patterson, A. Rinkevicius, A. Ryd, L. Skinnari, L. Soffi, W. Sun, S.M. Tan, W.D. Teo, J. Thom, J. Thompson, J. Tucker, Y. Weng, P. Wittich

Cornell University, Ithaca, USA

S. Abdullin, M. Albrow, G. Apollinari, S. Banerjee, L.A.T. Bauerdick, A. Beretvas, J. Berryhill, P.C. Bhat, G. Bolla, K. Burkett, J.N. Butler, H.W.K. Cheung, F. Chlebana, S. Cihangir, M. Cremonesi, V.D. Elvira, I. Fisk, J. Freeman, E. Gottschalk, L. Gray, D. Green, S. Grünendahl, O. Gutsche, D. Hare, R.M. Harris, S. Hasegawa, J. Hirschauer, Z. Hu, B. Jayatilaka, S. Jindariani, M. Johnson, U. Joshi, B. Klima, B. Kreis, S. Lammel, J. Lewis, J. Linacre, D. Lincoln, R. Lipton, T. Liu, R. Lopes De Sá, J. Lykken, K. Maeshima, J.M. Marraffino, S. Maruyama, D. Mason, P. McBride, P. Merkel, S. Mrenna, S. Nahn, C. Newman-Holmes [†], V. O'Dell, K. Pedro, O. Prokofyev, G. Rakness, E. Sexton-Kennedy, A. Soha, W.J. Spalding, L. Spiegel, S. Stoynev, N. Strobbe, L. Taylor, S. Tkaczyk, N.V. Tran, L. Uplegger, E.W. Vaandering, C. Vernieri, M. Verzocchi, R. Vidal, M. Wang, H.A. Weber, A. Whitbeck

Fermi National Accelerator Laboratory, Batavia, USA

D. Acosta, P. Avery, P. Bortignon, D. Bourilkov, A. Brinkerhoff, A. Carnes, M. Carver, D. Curry, S. Das, R.D. Field, I.K. Furic, J. Konigsberg, A. Korytov, K. Kotov, P. Ma, K. Matchev, H. Mei, P. Milenovic [67], G. Mitselmakher, D. Rank, R. Rossin, L. Shchutska, D. Sperka, N. Terentyev, L. Thomas, J. Wang, S. Wang, J. Yelton

University of Florida, Gainesville, USA

S. Linn, P. Markowitz, G. Martinez, J.L. Rodriguez

Florida International University, Miami, USA

A. Ackert, J.R. Adams, T. Adams, A. Askew, S. Bein, J. Bochenek, B. Diamond, J. Haas, S. Hagopian, V. Hagopian, K.F. Johnson, A. Khatiwada, H. Prosper, A. Santra, M. Weinberg

Florida State University, Tallahassee, USA

M.M. Baarmand, V. Bhopatkar, S. Colafranceschi [68], M. Hohlmann, H. Kalakhety, D. Noonan, T. Roy, F. Yumiceva

Florida Institute of Technology, Melbourne, USA

M.R. Adams, L. Apanasevich, D. Berry, R.R. Betts, I. Bucinskaite, R. Cavanaugh, O. Evdokimov, L. Gauthier, C.E. Gerber, D.J. Hofman, P. Kurt, C. O'Brien, I.D. Sandoval Gonzalez, P. Turner, N. Varelas, Z. Wu, M. Zakaria, J. Zhang

University of Illinois at Chicago (UIC), Chicago, USA

B. Bilki [69], W. Clarida, K. Dilsiz, S. Durgut, R.P. Gandrajula, M. Haytmyradov, V. Khristenko, J.-P. Merlo, H. Mermerkaya [70], A. Mestvirishvili, A. Moeller, J. Nachtman, H. Ogul, Y. Onel, F. Ozok [71], A. Penzo, C. Snyder, E. Tiras, J. Wetzel, K. Yi

The University of Iowa, Iowa City, USA

I. Anderson, B. Blumenfeld, A. Cocoros, N. Eminizer, D. Fehling, L. Feng, A.V. Gritsan, P. Maksimovic, M. Osherson, J. Roskes, U. Sarica, M. Swartz, M. Xiao, Y. Xin, C. You

Johns Hopkins University, Baltimore, USA

P. Baringer, A. Bean, C. Bruner, J. Castle, R.P. Kenny III, A. Kropivnitskaya, D. Majumder, M. Malek, W. Mcbrayer, M. Murray, S. Sanders, R. Stringer, Q. Wang

The University of Kansas, Lawrence, USA

A. Ivanov, K. Kaadze, S. Khalil, M. Makouski, Y. Maravin, A. Mohammadi, L.K. Saini, N. Skhirtladze, S. Toda

Kansas State University, Manhattan, USA

D. Lange, F. Rebassoo, D. Wright

Lawrence Livermore National Laboratory, Livermore, USA

C. Anelli, A. Baden, O. Baron, A. Belloni, B. Calvert, S.C. Eno, C. Ferraioli, J.A. Gomez, N.J. Hadley, S. Jabeen, R.G. Kellogg, T. Kolberg, J. Kunkle, Y. Lu, A.C. Mignerey, Y.H. Shin, A. Skuja, M.B. Tonjes, S.C. Tonwar

University of Maryland, College Park, USA

A. Apyan, R. Barbieri, A. Baty, R. Bi, K. Bierwagen, S. Brandt, W. Busza, I.A. Cali, Z. Demiragli, L. Di Matteo, G. Gomez Ceballos, M. Goncharov, D. Gulhan, D. Hsu, Y. Iiyama, G.M. Innocenti, M. Klute, D. Kovalskyi, K. Krajczar, Y.S. Lai, Y.-J. Lee, A. Levin, P.D. Luckey, A.C. Marini, C. Mcginn, C. Mironov, S. Narayanan, X. Niu, C. Paus, C. Roland, G. Roland, J. Salfeld-Nebgen, G.S.F. Stephans, K. Sumorok, K. Tatar, M. Varma, D. Velicanu, J. Veverka, J. Wang, T.W. Wang, B. Wyslouch, M. Yang, V. Zhukova

Massachusetts Institute of Technology, Cambridge, USA

A.C. Benvenuti, B. Dahmes, A. Evans, A. Finkel, A. Gude, P. Hansen, S. Kalafut, S.C. Kao, K. Klapoetke, Y. Kubota, Z. Lesko, J. Mans, S. Nourbakhsh, N. Ruckstuhl, R. Rusack, N. Tambe, J. Turkewitz

University of Minnesota, Minneapolis, USA

J.G. Acosta, S. Oliveros

University of Mississippi, Oxford, USA

E. Avdeeva, R. Bartek, K. Bloom, S. Bose, D.R. Claes, A. Dominguez, C. Fangmeier, R. Gonzalez Suarez, R. Kamalieddin, D. Knowlton, I. Kravchenko, F. Meier, J. Monroy, F. Ratnikov, J.E. Siado, G.R. Snow, B. Stieger

University of Nebraska-Lincoln, Lincoln, USA

M. Alyari, J. Dolen, J. George, A. Godshalk, C. Harrington, I. Iashvili, J. Kaisen, A. Kharchilava, A. Kumar, A. Parker, S. Rappoccio, B. Roozbahani

State University of New York at Buffalo, Buffalo, USA

G. Alverson, E. Barberis, D. Baumgartel, M. Chasco, A. Hortiangtham, A. Massironi, D.M. Morse, D. Nash, T. Orimoto, R. Teixeira De Lima, D. Trocino, R.-J. Wang, D. Wood, J. Zhang

Northeastern University, Boston, USA

S. Bhattacharya, K.A. Hahn, A. Kubik, J.F. Low, N. Mucia, N. Odell, B. Pollack, M.H. Schmitt, K. Sung, M. Trovato, M. Velasco

Northwestern University, Evanston, USA

N. Dev, M. Hildreth, C. Jessop, D.J. Karmgard, N. Kellams, K. Lannon, N. Marinelli, F. Meng, C. Mueller, Y. Musienko [39], M. Planer, A. Reinsvold, R. Ruchti, N. Rupprecht, G. Smith, S. Taroni, N. Valls, M. Wayne, M. Wolf, A. Woodard

University of Notre Dame, Notre Dame, USA

L. Antonelli, J. Brinson, B. Bylsma, L.S. Durkin, S. Flowers, A. Hart, C. Hill, R. Hughes, W. Ji, B. Liu, W. Luo, D. Puigh, M. Rodenburg, B.L. Winer, H.W. Wulsin

The Ohio State University, Columbus, USA

O. Driga, P. Elmer, J. Hardenbrook, P. Hebda, S.A. Koay, P. Lujan, D. Marlow, T. Medvedeva, M. Mooney, J. Olsen, C. Palmer, P. Piroué, D. Stickland, C. Tully, A. Zuranski

Princeton University, Princeton, USA

S. Malik

University of Puerto Rico, Mayaguez, USA

A. Barker, V.E. Barnes, D. Benedetti, L. Gutay, M.K. Jha, M. Jones, A.W. Jung, K. Jung, D.H. Miller, N. Neumeister, B.C. Radburn-Smith, X. Shi, J. Sun, A. Svyatkovskiy, F. Wang, W. Xie, L. Xu

Purdue University, West Lafayette, USA

N. Parashar, J. Stupak

Purdue University Calumet, Hammond, USA

A. Adair, B. Akgun, Z. Chen, K.M. Ecklund, F.J.M. Geurts, M. Guilbaud, W. Li, B. Michlin, M. Northup, B.P. Padley, R. Redjimi, J. Roberts, J. Rorie, Z. Tu, J. Zabel

Rice University, Houston, USA

B. Betchart, A. Bodek, P. de Barbaro, R. Demina, Y.t. Duh, Y. Eshaq, T. Ferbel, M. Galanti, A. Garcia-Bellido, J. Han, O. Hindrichs, A. Khukhunaishvili, K.H. Lo, P. Tan, M. Verzetti

University of Rochester, Rochester, USA

J.P. Chou, E. Contreras-Campana, Y. Gershtein, T.A. Gómez Espinosa, E. Halkiadakis, M. Heindl, D. Hidas, E. Hughes, S. Kaplan, R. Kunnawalkam Elayavalli, S. Kyriacou, A. Lath, K. Nash, H. Saka, S. Salur, S. Schnetzer, D. Sheffield, S. Somalwar, R. Stone, S. Thomas, P. Thomassen, M. Walker

Rutgers, The State University of New Jersey, Piscataway, USA

M. Foerster, J. Heideman, G. Riley, K. Rose, S. Spanier, K. Thapa

University of Tennessee, Knoxville, USA

O. Bouhali [72], A. Castaneda Hernandez [72], A. Celik, M. Dalchenko, M. De Mattia, A. Delgado, S. Dildick, R. Eusebi, J. Gilmore, T. Huang, T. Kamon [73], V. Krutelyov, R. Mueller, I. Osipenkov, Y. Pakhotin, R. Patel, A. Perloff, L. Perniè, D. Rathjens, A. Rose, A. Safonov, A. Tatarinov, K.A. Ulmer

Texas A&M University, College Station, USA

N. Akchurin, C. Cowden, J. Damgov, C. Dragoiu, P.R. Dudero, J. Faulkner, S. Kunori, K. Lamichhane, S.W. Lee, T. Libeiro, S. Undleeb, I. Volobouev, Z. Wang

Texas Tech University, Lubbock, USA

E. Appelt, A.G. Delannoy, S. Greene, A. Gurrola, R. Janjam, W. Johns, C. Maguire, Y. Mao, A. Melo, H. Ni, P. Sheldon, S. Tuo, J. Velkovska, Q. Xu

Vanderbilt University, Nashville, USA

M.W. Arenton, P. Barria, B. Cox, B. Francis, J. Goodell, R. Hirosky, A. Ledovskoy, H. Li, C. Neu, T. Sinthuprasith, X. Sun, Y. Wang, E. Wolfe, F. Xia

University of Virginia, Charlottesville, USA

C. Clarke, R. Harr, P.E. Karchin, C. Kottachchi Kankanamge Don, P. Lamichhane, J. Sturdy

Wayne State University, Detroit, USA

D.A. Belknap, D. Carlsmith, S. Dasu, L. Dodd, S. Duric, B. Gomber, M. Grothe, M. Herndon, A. Hervé, P. Klabbers, A. Lanaro, A. Levine, K. Long, R. Loveless, A. Mohapatra, I. Ojalvo, T. Perry, G.A. Pierro, G. Polese, T. Ruggles, T. Sarangi, A. Savin, A. Sharma, N. Smith, W.H. Smith, D. Taylor, P. Verwilligen, N. Woods

University of Wisconsin – Madison, Madison, WI, USA

† Deceased.
[1] Also at Vienna University of Technology, Vienna, Austria.
[2] Also at State Key Laboratory of Nuclear Physics and Technology, Peking University, Beijing, China.
[3] Also at Institut Pluridisciplinaire Hubert Curien, Université de Strasbourg, Université de Haute Alsace Mulhouse, CNRS/IN2P3, Strasbourg, France.
[4] Also at Universidade Estadual de Campinas, Campinas, Brazil.
[5] Also at Centre National de la Recherche Scientifique (CNRS) – IN2P3, Paris, France.
[6] Also at Université Libre de Bruxelles, Bruxelles, Belgium.
[7] Also at Laboratoire Leprince-Ringuet, Ecole Polytechnique, IN2P3-CNRS, Palaiseau, France.
[8] Also at Joint Institute for Nuclear Research, Dubna, Russia.
[9] Also at Suez University, Suez, Egypt.
[10] Now at British University in Egypt, Cairo, Egypt.
[11] Also at Ain Shams University, Cairo, Egypt.
[12] Also at Cairo University, Cairo, Egypt.
[13] Now at Helwan University, Cairo, Egypt.
[14] Also at Université de Haute Alsace, Mulhouse, France.
[15] Also at CERN, European Organization for Nuclear Research, Geneva, Switzerland.
[16] Also at Skobeltsyn Institute of Nuclear Physics, Lomonosov Moscow State University, Moscow, Russia.
[17] Also at Tbilisi State University, Tbilisi, Georgia.
[18] Also at RWTH Aachen University, III. Physikalisches Institut A, Aachen, Germany.
[19] Also at University of Hamburg, Hamburg, Germany.
[20] Also at Brandenburg University of Technology, Cottbus, Germany.
[21] Also at Institute of Nuclear Research ATOMKI, Debrecen, Hungary.
[22] Also at MTA-ELTE Lendület CMS Particle and Nuclear Physics Group, Eötvös Loránd University, Budapest, Hungary.
[23] Also at University of Debrecen, Debrecen, Hungary.
[24] Also at Indian Institute of Science Education and Research, Bhopal, India.
[25] Also at University of Visva-Bharati, Santiniketan, India.
[26] Now at King Abdulaziz University, Jeddah, Saudi Arabia.
[27] Also at University of Ruhuna, Matara, Sri Lanka.
[28] Also at Isfahan University of Technology, Isfahan, Iran.
[29] Also at University of Tehran, Department of Engineering Science, Tehran, Iran.
[30] Also at Plasma Physics Research Center, Science and Research Branch, Islamic Azad University, Tehran, Iran.
[31] Also at Laboratori Nazionali di Legnaro dell'INFN, Legnaro, Italy.
[32] Also at Università degli Studi di Siena, Siena, Italy.
[33] Also at Purdue University, West Lafayette, USA.
[34] Now at Hanyang University, Seoul, Korea.
[35] Also at International Islamic University of Malaysia, Kuala Lumpur, Malaysia.
[36] Also at Malaysian Nuclear Agency, MOSTI, Kajang, Malaysia.
[37] Also at Consejo Nacional de Ciencia y Tecnología, Mexico city, Mexico.
[38] Also at Warsaw University of Technology, Institute of Electronic Systems, Warsaw, Poland.
[39] Also at Institute for Nuclear Research, Moscow, Russia.
[40] Now at National Research Nuclear University 'Moscow Engineering Physics Institute' (MEPhI), Moscow, Russia.

[41] Also at St. Petersburg State Polytechnical University, St. Petersburg, Russia.
[42] Also at University of Florida, Gainesville, USA.
[43] Also at Faculty of Physics, University of Belgrade, Belgrade, Serbia.
[44] Also at INFN Sezione di Roma; Università di Roma, Roma, Italy.
[45] Also at National Technical University of Athens, Athens, Greece.
[46] Also at Scuola Normale e Sezione dell'INFN, Pisa, Italy.
[47] Also at National and Kapodistrian University of Athens, Athens, Greece.
[48] Also at Riga Technical University, Riga, Latvia.
[49] Also at Institute for Theoretical and Experimental Physics, Moscow, Russia.
[50] Also at Albert Einstein Center for Fundamental Physics, Bern, Switzerland.
[51] Also at Adiyaman University, Adiyaman, Turkey.
[52] Also at Mersin University, Mersin, Turkey.
[53] Also at Cag University, Mersin, Turkey.
[54] Also at Piri Reis University, Istanbul, Turkey.
[55] Also at Gaziosmanpasa University, Tokat, Turkey.
[56] Also at Ozyegin University, Istanbul, Turkey.
[57] Also at Izmir Institute of Technology, Izmir, Turkey.
[58] Also at Marmara University, Istanbul, Turkey.
[59] Also at Kafkas University, Kars, Turkey.
[60] Also at Istanbul Bilgi University, Istanbul, Turkey.
[61] Also at Yildiz Technical University, Istanbul, Turkey.
[62] Also at Hacettepe University, Ankara, Turkey.
[63] Also at Rutherford Appleton Laboratory, Didcot, United Kingdom.
[64] Also at School of Physics and Astronomy, University of Southampton, Southampton, United Kingdom.
[65] Also at Instituto de Astrofísica de Canarias, La Laguna, Spain.
[66] Also at Utah Valley University, Orem, USA.
[67] Also at University of Belgrade, Faculty of Physics and Vinca Institute of Nuclear Sciences, Belgrade, Serbia.
[68] Also at Facoltà Ingegneria, Università di Roma, Roma, Italy.
[69] Also at Argonne National Laboratory, Argonne, USA.
[70] Also at Erzincan University, Erzincan, Turkey.
[71] Also at Mimar Sinan University, Istanbul, Istanbul, Turkey.
[72] Also at Texas A&M University at Qatar, Doha, Qatar.
[73] Also at Kyungpook National University, Daegu, Korea.